Carbonaceous Material Fractions in Sediments and Their Effect on the Sorption and Persistence of Organic Pollutants in Small Urban Watersheds

A research project funded by
Illinois Water Resources Center
Matching Grants Program
Grant No. 04HQGR0158

Project Final Report

By

Charles J. Werth
Department of Civil and Environmental Engineering
University of Illinois at Urbana-Champaign, Urbana, IL

Yaning Yang
Department of Civil and Environmental Engineering
University of Illinois at Urbana-Champaign, Urbana, IL

Peter C. Van Metre
U. S. Geological Survey, Austin, TX

Barbara J. Mahler
U. S. Geological Survey, Austin, TX

Department of Civil and Environmental Engineering
University of Illinois at Urbana-Champaign
May 29, 2009

TABLE OF CONTENTS

List of Tables

List of Figures

Chapter 1

1.1 Introduction

Long-term non-point source pollution caused by particle-associated contaminants (PACs) in urban lakes and streams is a common problem in the United States. PACs, including chlorinated organic compounds, trace elements, and polycyclic aromatic hydrocarbons (PAHs), are a major concern regarding public health and environmental impact because many of them are persistent, bioaccumulative and (or) toxic. The strong binding of PACs to particles and their subsequent slow release impact the bioavailability of contaminants, sediment quality, surface water quality, and remediation efforts. The occurrence of PACs has resulted in the impairment of thousands of streams, lakes, and reservoirs: PACs were responsible for fish-consumption advisories for 23 percent of total lake acreage and 9.3 percent of total river mileage in the United States in 2000 (USEPA, 2001), and PACs comprise more than 20 percent of total maximum daily loads (TMDLs) nationwide (USEPA, 2003).

Since 1991, the United States Geological Survey (USGS) National Water Quality Assessment (NAWQA) Program has been using sediment cores from reservoirs and lakes to define historical trends of PACs in urban and reference settings across the country, and investigating the extent to which the contaminant concentrations and trends recorded in sediment cores were associated with suspended sediment in influent streams (Van Metre et al., 1997, 2004). Van Metre and Mahler (2004) indicated that in small urban watersheds, concentrations of some PACs on suspended sediment in influent streams can greatly exceed those in bed sediments in the downstream reservoir, and that trend may not be preserved in cores for some PACs. Their observations present a problem for

effective sediment monitoring and highlight the difficulties encountered in using sediment cores to infer stream water quality. Although the significant loss of contaminants during transport and soon after deposition has been attributed to the solubilization of some contaminants, and the solubilization and mineralization of some solid-phase carbonaceous materials (CMs), relatively little is known about the role played by CMs in the transport and fate of PACs in small urban watersheds.

PACs of concern in this study are polycyclic aromatic hydrocarbons (PAHs) because of their high concentrations and widespread occurrence in the environment, as well as carcinogenic and mutagenic properties. Over the past 25 years, concentrations of PAHs have increased in many urban lakes and streams, particularly in areas with rapid urbanization (Van Metre et al., 1997, 2000; Van Metre and Mahler, 2005). PAHs strongly sorb to solid particles and enter receiving water bodies with storm runoff from impervious surfaces or storm sewers in urban watersheds, as well as by atmospheric deposition. We hypothesize that CM particles are the primary carriers of PAHs in urban watersheds and control the persistence of PAHs as they undergo transport from the land surface into receiving water bodies, and deposition and burial as sediments.

The overall objective of this study is to determine how CMs affect the fate and persistence of PACs in small urban watersheds, with a focus on PAHs. This will be achieved by correlation of the amount, type, and PAH sorption properties of CMs found in terrestrial and lake sediment particles of a watershed, where the former, via runoff, are a primary source of CMs and PAHs in lake sediments. Herein, terrestrial particles include street dust, sealed and unsealed parking lot dust, and residential and commercial soils.

This report contains a complete documentation of the research activities and outcomes. **Chapter 2** describes the sample collection, PAH concentrations in samples, and the distribution of CMs in urban watershed determined by organic petrography. The correlation between PAHs and CMs and the potential contribution of coal tar to PAHs are also presented. **Chapter 3** presents the results of chemical and thermal oxidation of field samples, and reference asphalt and coal tar materials, and compares the black carbon contents from these methods to those determined by organic petrography. **Chapter 4** presents the results of CM characterization in terms of element composition, surface functional groups, and specific surface area, and the sorption of phenanthrene to samples and subsamples. The main body of the report is followed by Appendices A, B, and C.

1.2 References

U.S. Environmental Protection Agency (USEPA), 2001, Update: National listing of fish and wildlife advisories. EPA-823-F-01-010.

U.S. Environmental Protection Agency (USEPA), 2003, http://oaspub.epa.gov/waters/national_rept.control, updated February 21st, 2003 (accessed February 21, 2003).

Van Metre, P.C., E. Callender, C.C. Fuller, 1997, Historical trends in organochlorine compounds in river basins identified using sediment cores from reservoirs. Environmental Science & Technology, 31, 2339-2344.

Van Metre, P.C., B.J. Mahler, 2004, Contaminant trends in reservoir sediment cores as records of influent stream quality. Environmental Science & Technology, 38, 2978-2986.

Van Metre, P.C., J.T. Wilson, C.C. Fuller, E. Callender, B.J. Mahler, 2004, Collection, analysis, and age dating of sediment cores from 56 U.S. lakes and reservoirs sampled by the U.S. Geological Survey, 1992-2001: U.S. Geological Survey Scientific Investigations Report SIR 2004-5184, 180p.

Van Metre, P.C., B.J. Mahler, 2005, Trends in hydrophobic organic contaminants in urban and reference lake sediments across the United States, 1970-2001. Environmental Science & Technology, 39, 5567-5574.

Chapter 2

The Influence of Coal-Tar Sealant and Other Carbonaceous Materials on Polycyclic Aromatic Hydrocarbon Loads in an Urban Watershed

2.1 Introduction

Polycyclic aromatic hydrocarbons (PAHs) are common contaminants in the environment. Many PAHs and their metabolites are toxic, mutagenic, and/or carcinogenic, and adversely affect human health and aquatic ecosystems. Over the past 30 years, total PAH concentrations (∑PAH) in urban fresh-water sediments generally have increased (Mahler et al., 2005; Van Metre and Mahler, 2005; Chalmers et al., 2007) and increasing ∑PAH are correlated with increases in urban land-use intensity (Van Metre and Mahler, 2005; Chalmers et al., 2007). Numerous urban sources of PAHs have been identified, including the combustion of fossil fuels, forest fires, motor oil, tire debris, roofing tar, asphalt pavement, and coal tar (Wakeham et al., 1980; Rogge et al., 1993a, 1993b, 1997, 1998; Breedveld et al., 2007). Surface runoff is the most important pathway for the introduction of PAHs into aquatic environments in small urban watersheds (Van Metre and Mahler, 2004; Kimbrough and Dickhut, 2006; Chalmers et al., 2007) and the majority of PAHs in runoff are associated with carbonaceous material (CM) particles (Motelay-Massei et al., 2006). However, the role of CM particles as PAH sources and carriers in urban streams and lakes remains unclear.

CM particles in urban runoff originate from different land-use settings, including residential and commercial soils, rooftops, roads, parking lots, and construction sites. They are derived from heterogeneous source materials, for example, recently accumulated organic debris of plants and animals, partially humified materials,

geopolymers such as kerogen and coal, various types of char and soot from combustion of fuel and biomass, and coal and petroleum byproducts (Murakami et al., 2005; Jeong et al., 2008). The latter can be released from vehicles and industries and by the wear of tires and of asphalt-paved and coal-tar-sealed infrastructure surfaces (Mahler et al., 2005, Murakami et al., 2005). All of these source materials can be altered in the environment by physical, chemical, and biological processes. In recent years, efforts have been made to measure PAH concentrations in a variety of CM particles, including combustion-derived soot (Gustafsson et al., 1997; Jonker et al., 2005) and charcoal (Jonker et al., 2005), and coal-and-petroleum-derived CMs such as coal (Jonker et al., 2005), coke (Khalili et al., 1995), coal tar (Khalil et al., 2006), and asphalt (Wakeham et al., 1980). Several particulate CMs have been found to be important sources of PAHs in urban environments. Boonyatumanond et al. (2007) reported that tire debris was the major contributor of PAHs to street dust in Bangkok, Thailand. Murakami et al. (2008) found that pyrogenic CM particles including diesel exhaust were the dominant source of PAHs in runoff from Chuo Highway in Tokyo, Japan. Because methods used in source apportionment are generally limited to PAH profile measurements with statistical analysis, the types, amounts, and origins of PAH-associated CM particles in urban stream and lake sediments are unknown.

Mahler et al. (2005) found that particles in simulated runoff from parking lots treated with coal-tar-based sealcoat had an average 65-times higher ∑PAH (mean of 3,500 mg/kg) than those from unsealed asphalt and concrete parking lots. Similarly, Van Metre et al. (2009) found that PAH concentrations in dust swept from sealed parking lots in the central and eastern U.S., where coal-tar sealcoat is used, were about 1,000 times

higher than those in dust swept from sealed parking lots in western U.S., where asphalt-based sealcoat is used (median concentrations of 2,200 and 2.1 mg/kg, respectively). The concentrations in particles from coal-tar-sealed pavements were one to two orders of magnitude higher than those in tire wear particles in Bangkok (Boonyatumanond et al., 2007), and about 15 times higher than those in diesel vehicle exhaust particles in Tokyo (Murakami et al., 2008). To our knowledge, coal-tar sealants are not in use in Japan or Thailand. Values for national use of coal-tar sealcoat in the U.S. are not available, but the sealcoat industry estimates that in the State of Texas, 225 million L of refined coal-tar-based sealcoat are applied annually (Scoggins et al., 2007 and references therein), and the New York Academy of Sciences reported estimated annual use of coal-tar-based sealcoat in the New York harbor watershed of approximately 5.3 million L (Valle, 2007). Mass balance estimates and PAH assemblages indicate that runoff from parking lots treated with coal-tar sealcoat is a major source of PAHs in the urban watersheds studied (Mahler et al., 2005). Although it is clear that coal-tar sealcoat contributes to PAHs in urban stream and lake sediments, there remains considerable uncertainty regarding the specific contributions of this CM to PAH loadings, and to the fate of PAHs associated with coal tar sealcoats.

In this study, for the Lake Como watershed in Fort Worth, Texas, we characterized CM particles and PAHs in soils and in dust from paved surfaces that likely are mobilized by runoff, and in sediment from the reservoir and its influent stream. CM particles were characterized using organic petrography, and these characteristics were compared to PAH concentrations to identify the types of CMs that are the principal contributors to PAH loadings in the urban reservoir. The objectives are to identify the

sources and distribution of CM particles in this small urban watershed and to determine which CMs are the dominant sources of PAHs in the lake and stream sediments, with a focus on the role of coal-tar sealants used on parking lots. Information on the association of PAHs with CM particles in urban runoff will contribute to the assessment of the fate of PAHs and their influence on aquatic environments and the development of watershed management strategies to control PAH contamination and improve water quality.

2.2 Materials and Methods

Details of sampling and analytical methods and all PAH data are presented in Wilson et al. (2006), and are summarized briefly here. Note that only residential soil #1 reported in Wilson et al. (2006) was used in our study.

2.2.1 Sample Collection

Samples of sediment, soil, and pavement dust were collected in October 2004 from the Lake Como watershed in Fort Worth, Texas (Figure A1, Appendix A). The watershed is 2.75 km^2 in area, of which 90.4% is urbanized. About one-half of the developed land is residential (47.6%) and one- half is commercial, industrial, and transportation (Van Metre et al., 2003 and references therein). Three sediment cores were collected from a single site in Lake Como using a box corer. The site corresponds to the lower lake site in Van Metre et al. (2003), and cores were taken several meters apart to avoid sampling of disturbed sediment. The cores were vertically extended and sliced at 5-cm intervals, and subsamples from similar depths (depth from the top: 0-5 cm, 10-15 cm, and 25-30 cm) were combined from the three cores to create three large-volume samples.

Influent suspended-sediment samples were obtained by filtering 75 L of stormwater collected from the influent stream during a runoff event through a 0.45-µm PTFE-membrane (Mahler and Van Metre, 2003). The sampling site is the same as was monitored for suspended-sediment chemistry and loads by Van Metre et al. (2003). Influent streambed sediment samples were collected with a stainless steel scoop at the same locations as the suspended-sediment three days following the storm event during which the suspended-sediment samples had been collected. Streambed sediment samples were collected from areas of the channel where fine-grained sediment had accumulated by scooping the soft, relatively fine-grained top sediment. Numerous scoops were combined to obtain a composite sample. Two composite surface soil samples, one from a residential neighborhood and the other from a commercial area, were collected by random sampling at approximately 40 locations near roads, sidewalks, and driveways using stainless steel scoops. One composite residential street dust sample was collected from three asphalt-paved residential streets using nylon push brooms and stainless steel dust pans. Two composite parking lot dust samples were collected; one was composited from dust from three coal-tar-sealed commercial parking lots and the other was composited from dust from three unsealed asphalt or cement commercial parking lots. Each sample of streambed sediment, soil, and pavement dust was homogenized and split after passing through a 1-mm sieve; one part was sent to the University of Illinois at Urbana-Champaign (UIUC) and the other part was sent to the USGS laboratory in Denver, Colorado.

2.2.2 Sample Characterization

Sediment deposition dates for lake sediment samples were estimated on the basis of the sedimentation rate in an age-dated core collected at the same location in 2001 (Van Metre et al., 2003). Total CM contents were estimated by measuring weight loss after heating samples at 550ºC for 4 h in a Thermolyne F62700 muffle furnace (Barnstead International) (Heiri et al., 2001). Total organic carbon (TOC) contents were determined with a CE 440 CHN analyzer (Exeter Analytical, Inc.) in the Microanalysis Laboratory at UIUC.

2.2.3 Organic Petrography

Quantitative petrographic analysis was performed on all samples except the suspended-sediment (because of insufficient sample mass) after the removal of carbonate and silicate minerals by treatment with HCl/HF. CM-enriched samples first were embedded on the surface of a liquid epoxy resin, which was subsequently hardened. Resin surfaces were polished and the embedded CMs were observed with a Leitz DMRX-MPVSP photometer microscope using reflected white light and UV+violet-light illumination (fluorescence mode). CM particles were identified and classified according to maceral groups and their subgroups as defined by Taylor et al. (1998). Maceral volume fractions in each sample were determined by point counting of at least 500 macerals using a multi-point cross-hair ocular. The overall accuracy has been determined to be approximately ±2% (Taylor et al., 1998). Three types of CM particles were physically separated by picking with tweezers from representative samples for microscale PAH extraction and analysis: recent organic matter (OM) from residential soil, asphalt- and bitumen-like substances from unsealed parking lot dust, and coal-tar pitch from sealed

parking lot dust. The latter two particle types could not reasonably be picked from other samples because of their small volume fractions.

2.2.4 PAH Analysis

Eighteen parent PAHs, nine specific alkyl-PAHs, and the homologous series of alkyl-PAHs in bulk samples were determined at the USGS laboratory (Olson et al., 2003). Briefly, samples were extracted overnight with dichloromethane in a Soxhlet apparatus. The extracts were injected into a polystyrene-divinylbenzene gel permeation column and eluted with dichloromethane to remove sulfur and partially isolate the target analytes. PAHs and alkyl-PAHs were analyzed by gas chromatography (GC) with mass spectrometry (MS). Separated CM particles were extracted with acetone and dichromathane by accelerated solvent extraction (ASE) at UIUC (EPA method 3545). The extract was cleaned with silica gel (EPA method 3630c), and 16 EPA priority PAHs were analyzed with GC/MS following EPA method 8270c. Quality assurance was provided by analyzing duplicate samples, laboratory blanks, and spiked reagent samples, and monitoring recovery of surrogate compounds. The sum of 13 PAHs in bulk samples ($\sum_{13}\mathrm{PAH}$) are reported here to compare with the consensus-based sediment-quality-guideline (SQG) probable effect concentration (PEC) (MacDonald et al., 2000). For consistency with literature values of PAHs on specific CM particles, the sum of 11 PAHs ($\sum_{11}\mathrm{PAH}$) on separated particles was used.

2.2.5 Data Analysis

Mass percentages of different CMs in each sample were estimated from measured volume fractions and densities determined from the literature or in our laboratory. Organic carbon (OC) contributions of different CMs in each sample were estimated from the calculated mass percentages, OC contents of CMs determined from the literature or in our laboratory, and the measured TOC of bulk samples. Potential PAH loading from coal-tar pitch and the distribution of PAHs among all types of CMs were calculated using PAH concentrations in CM particles determined from the literature or measured in our laboratory. The uncertainty analysis for predicted parameters was estimated by Monte Carlo simulation with Crystal Ball 2000 (Oracle Corp.). The resulting distribution of simulated output was analyzed by least trimmed squares regression with Systat 12 (Systat Software, Inc.) to eliminate the outliers. The estimated means are reported. Details of the risk analysis are in the Appendix A.

2.3 Results and Discussion

2.3.1 PAH Concentrations

Concentrations of $\sum_{13} \mathrm{PAH}$ varied over about three orders of magnitude, with the largest concentrations in the dust from sealed parking lots (Figure 2.1). The $\sum_{13} \mathrm{PAH}$ concentration in that sample (980 mg/kg) greatly exceeds concentrations in all other urban dust and soils; it is about 2000 times greater than that in residential soil (0.49 mg/kg), 1500 times greater than in residential street dust (0.65 mg/kg), and 30 times

greater than in unsealed parking lot dust (32 mg/kg). Stream and lake sediments show a pattern similar to previous studies (Van Metre and Mahler, 2004), with the suspended-sediment concentration of $\sum_{13}\text{PAH}$ (43 mg/kg) higher than streambed sediment (11 mg/kg), and streambed sediment higher than lake sediments (5.7 to 10 mg/kg). This relation likely results from the loss of PAHs to desorption and solubilization of OM during transport and early diagenesis and the dilution of bottom sediment by cleaner coarser material (especially in the streambed). For comparison, the consensus-based sediment-quality-guideline probable effect concentration (PEC) for $\sum_{13}\text{PAH}$ in fresh water aquatic sediments, i.e., the level above which adverse biological effects are expected to occur, is 22.8 mg/kg (MacDonald et al., 2000).

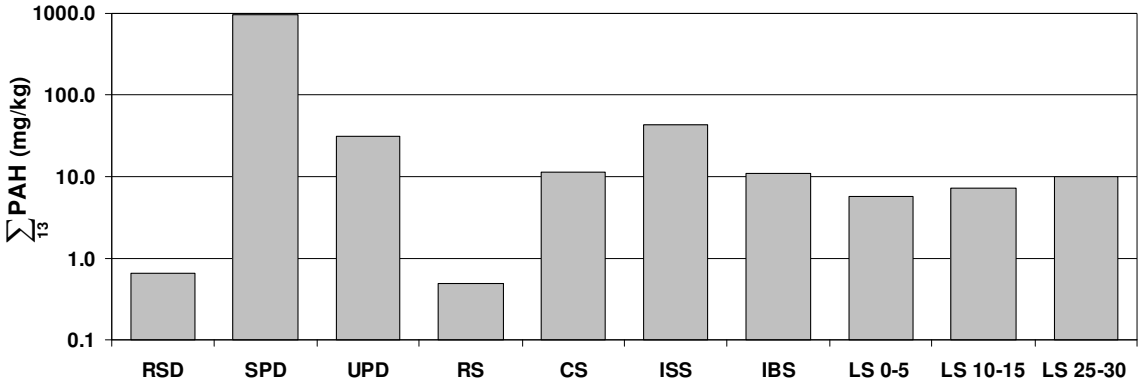

Figure 2.1. Total PAH concentrations in Lake Como watershed samples. Samples include residential street dust (RSD), sealed parking lot dust (SPD), unsealed parking lot dust (UPD), residential soil (RS), commercial soil (CS), influent suspended-sediment (ISS), influent bed sediment (IBS), lake sediment from 0-5 cm depth (LS 0-5), lake sediment from 10-15 cm depth (LS 15-20), and lake sediment from 25-30 cm depth (LS 25-30). ($\sum_{13}\text{PAH}$ as used here is the sum of the detected and estimated concentrations of 13 PAHs as used in the consensus based SQG (MacDonald et al., 2000): naphthalene, 2-methylnaphthalene, acenaphthylene, acenaphthene, 9H-fluorene, phenanthrene, anthracene, fluoranthene, pyrene, benz(a)anthracene, chrysene, dibenzo(a,h)anthracene, and benzo(a)pyrene.)

The $\sum_{13} PAH$ concentrations increase in lake sediments with depth, meaning they are lower in recent years; the 25-30 cm interval is estimated to be about 6 years old (deposited in about 1998). The decrease in PAH concentrations over the past several years might indicate a decrease in PAH load from the watershed but also could be caused by an increase in erosion of cleaner sediment from the watershed (dilution).

The $\sum_{11} PAH$ concentration in recent OM particles separated from residential soil is 68 mg/kg (Table A3, Appendix A), which is lower than that measured by Ahn et al. (2005) (170 mg/kg) and Khalil et al. (2006) (990 mg/kg), who analyzed particles from contaminated coke oven site soil and manufactured gas plant (MGP) site sediment, respectively. PAHs in separated asphalt- and bitumen-like substances and coal-tar pitch are 2,850 and 75,000 mg/kg, respectively, similar to those detected in asphalt-based and coal-tar-based sealant (2,900 and 87,000 mg/kg, respectively) (Mahler et al., 2005) and coal tar particles from the MGP site (53,000 mg/kg) (Khalil et al., 2006).

2.3.2 Organic Petrography

Identified macerals in samples, which consist of multiple subgroups with different physical appearance and volume fractions, are classified into two categories: Recent OM and CMs resulting from anthropogenic contamination (Table A1, Appendix A). Recent OM comprises the following maceral groups: huminite, vitrinite, liptinite, and inertinite. CMs resulting from anthropogenic contamination include hard coal, coke, char, soot, and coal- and petroleum-derived fluorescent materials such as coal-tar pitch and asphalt- and bitumen-like substances. Morphologies of various CM particles such as recent OM, coal, char, and coal-tar pitch in soil or sediment samples have been presented elsewhere

(Karapanagioti et al., 2000; Ghosh et al., 2003), thus, only photographs of representative anthropogenic CM particles in selected samples are presented here (Figure A2, Appendix A).

Recent OM, asphalt- and bitumen-like substances, and soot were found in all samples, while hard coal, char, and coke were often below the detection limit (0.2 vol % for particles greater than 1 to 2 microns) and never exceeded 1.0 % (Table A1, Appendix A). Estimation of mean mass percentages of CMs in each sample indicates that recent OM dominates all soil and sediment samples, ranging from 52.4% to 79.0% (Figure 2.2). The fractions of soot are higher in lake sediments and unsealed parking lot dust than in other samples, ranging from 17.3 to 20.9%. Asphalt- and bitumen-like substances dominate unsealed parking lot dust (50.9%), and are a major component of residential street dust (45.1%), along with recent OM (43.7%). The fraction of asphalt- and bitumen-like substances decreases progressively from unsealed parking lot and residential street dust, to streambed sediment (36.1%), to lake sediments (5.1-11.1%). This suggests that these particles are transported to the lake with runoff, diluted by other CM particles, and possibly removed/degraded over time in buried sediments.

Coal-tar pitch was found in six samples, and its percent contribution varies widely. It dominates sealed parking lot dust (57.5%), and is a small part of unsealed parking lot dust, commercial soil, surficial lake sediment, and streambed sediment (7.8%, 3.6%, 3.2%, and 1.4%). Occurrence of coal-tar pitch in unsealed parking lot dust and commercial soil likely result from offsite transport from sealed parking lots by vehicle or wind (Van Metre et al., 2009). Coal-tar pitch in streambed sediment and surficial lake

sediment likely results from runoff from parking lots. Coal-tar pitch either was not detected or was detected at a very low proportion in lake sediment at lower depths (Table A1, Appendix A). This suggests that (1) runoff of coal-tar particles has increased in recent years, (2) runoff of other particle types relative to coal tar has decreased in recent years, and/or that (3) coal-tar particles are unstable in water and are removed/degraded with time.

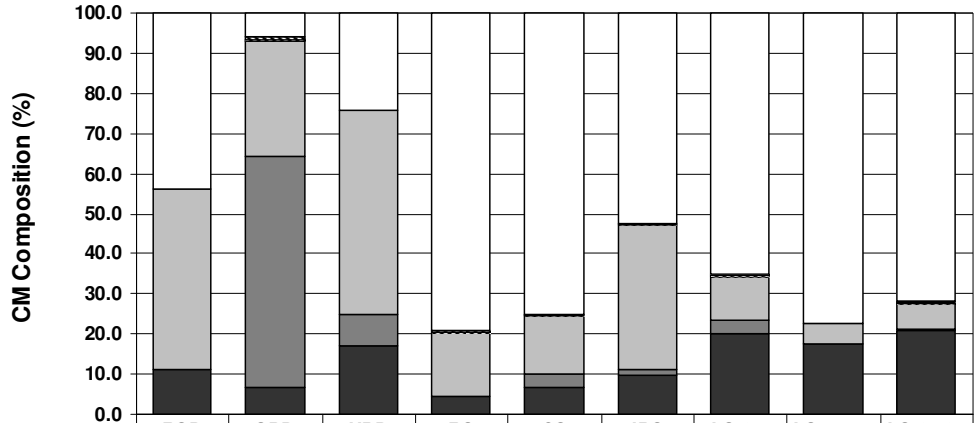

	RSD	SPD	UPD	RS	CS	IBS	LS 0-5	LS 10-15	LS 25-30
Recent OM	43.7	5.8	24.0	79.0	75.0	52.4	65.1	77.3	71.7
Hard Coal	0.0	0.8	0.0	0.3	0.3	0.0	0.3	0.0	0.5
Char	0.0	0.0	0.0	0.0	0.0	0.0	0.0	0.1	0.0
Coke	0.0	0.3	0.0	0.3	0.0	0.3	0.3	0.0	0.3
Asphalt- and Bitumen-like Substances	45.1	29.0	50.9	15.8	14.5	36.1	11.1	5.1	6.2
Coal-Tar Pitch	0.0	57.5	7.8	0.0	3.6	1.4	3.2	0.0	0.4
Soot	11.2	6.7	17.3	4.5	6.6	9.8	20.1	17.5	20.9

Figure 2.2. Mass percentages of carbonaceous materials (CMs) in Lake Como watershed samples.

2.3.3 Distribution of OC

The TOC and OC contributed by different types of CMs vary among samples (Table 2.1). The distribution of OC among CMs in samples also is different (Figure A3,

Table 2.1. TOC and OC contributed by CMs in Lake Como watershed samples.

Sample	TOC (g OC/100g bulk sample)	OC Contributed by CMi in Sample (g OC/100g bulk sample)						
		Recent OM	Hard Coal	Coke	Char	Soot	Asphalt- and Bitumen-like Substances	Coal-Tar Pitch
RSD	2.87±0.18	1.21±0.09	0.00	0.00	0.00	0.23±0.07	1.42±0.11	0.00
SPD	4.20±0.29	0.24±0.04	0.04±0.02	0.02*	0.00	0.22±0.07	1.49±0.11	2.18±0.18
UPD	2.78±0.25	0.63±0.07	0.00	0.00	0.00	0.35±0.09	1.60±0.16	0.18±0.02
RS	2.80±0.13	2.16±0.11	0.01*	0.01*	0.00	0.10±0.02	0.52±0.04	0.00
CS	4.00±0.07	2.96±0.09	0.01*	0.00	0.00	0.20±0.07	0.69±0.07	0.13±0.02
IBS	2.22±0.02	1.12±0.04	0.00	0.01*	0.00	0.16±0.04	0.91±0.04	0.03*
LS 0-5	3.92±0.06	2.65±0.13	0.01*	0.02*	0.00	0.61±0.13	0.53±0.04	0.11±0.02
LS 10-15	4.71±0.23	3.77±0.25	0.00	0.01*	0.00	0.64±0.16	0.29±0.04	0.00
LS 25-30	5.04±0.14	3.75±0.18	0.03±0.02	0.02*	0.00	0.84±0.20	0.39±0.04	0.02*

* Standard deviation is below 0.005.

Appendix A). The TOC contents in lake sediments are 3.92, 4.71, and 5.04 g OC/100 g bulk sample for depths of 0-5 cm, 10-15cm, and 25-30cm, respectively, and the increasing trend suggests greater accumulation of OM in sediments in past years. These values are higher than that for the bed sediment in the influent stream (2.22 g OC/100 g bulk sample), indicating that lake sediment acts as a sink for CMs. Two processes likely contribute to the increase in TOC in lake sediment relative to streambed sediment. Lake sediment is very fine grained and OC correlates to percent fines in aquatic sediments (Horowitz and Elrick, 1987), suggesting less dilution of OC in lake sediment by coarser material relative to streambed sediment. Secondly, autochthonous production of organic matter in the lake contributes to OM in lake sediments. The OC contributed by different types of CMs in each sample generally mirrors results for mass percentages of CMs in each sample presented in Figure 2.2, with small relative differences in percent contributions.

2.3.4 Correlations between PAHs and CMs

To investigate the relations between CMs and PAHs, logarithm values of total PAHs ($\log(\sum_{13}\text{PAH})$), high molecular weight (HMW) PAHs, and low molecular weight (LMW) PAHs in samples were plotted against OC contents of selected CMs (Figure 2.3). Extensive research has shown positive correlations between ∑PAH and TOC or soot carbon (SC) in soil and sediment samples (Tsapakis et al., 2003; Zhang et al., 2004), but no correlation was observed between $\log(\sum_{13}\text{PAH})$ and TOC or SC here (Figure 2.3a and 2.3b). However, values of $\log(\sum_{13}\text{PAH})$ are positively correlated to the sum of OC in soot, coal tar, and asphalt- and bitumen-like substances ($R^2 = 0.66$), and this correlation is

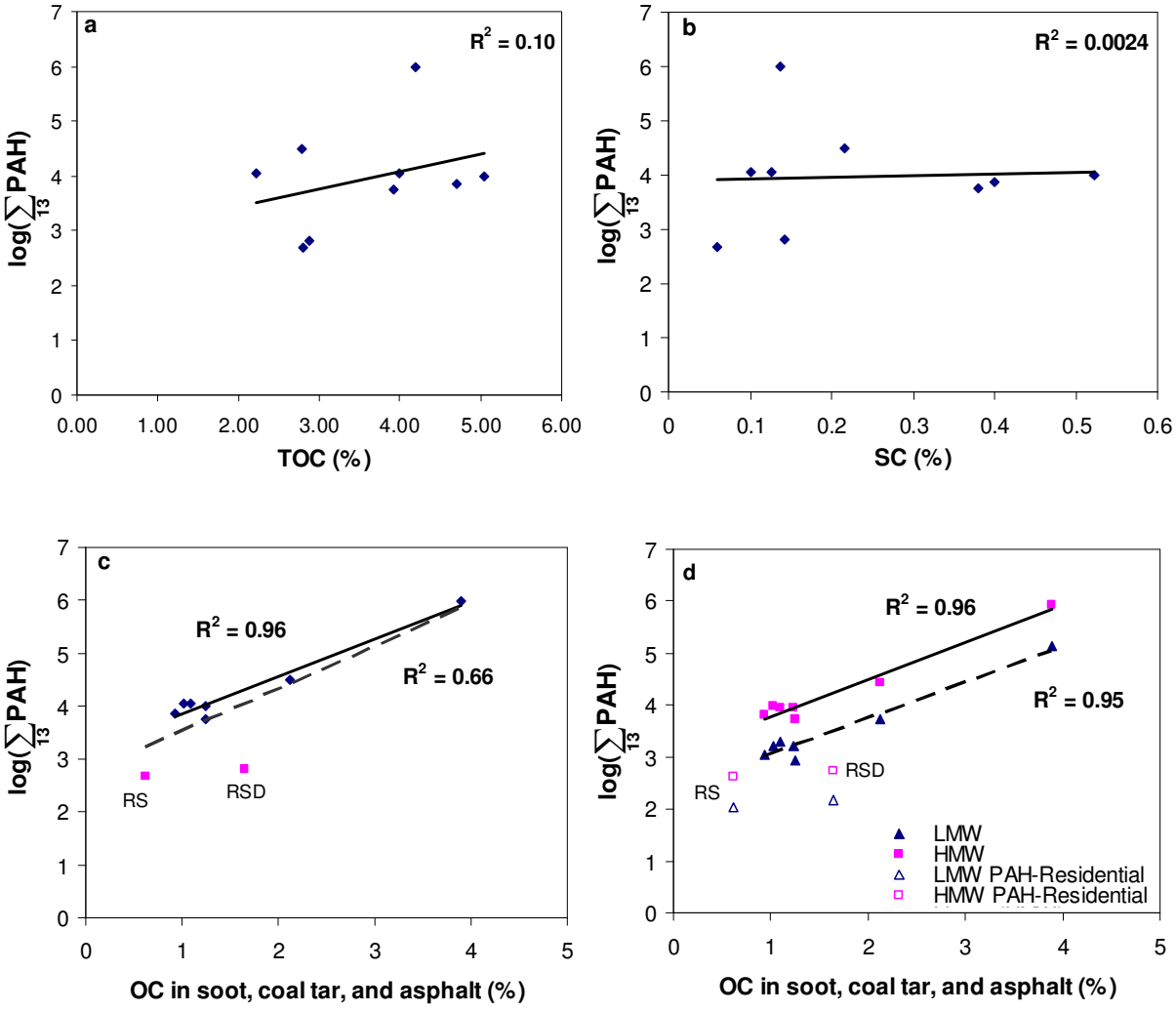

Figure 2.3. Correlations between total PAHs and organic carbon (OC) contents in different CMs in Lake Como watershed samples: (a) TOC vs. $\log(\sum_{13}\text{PAH})$; (b) SC vs. $\log(\sum_{13}\text{PAH})$ (SC is determined using the ratio of f_{sc} and f_{oc} in diesel soot (SRM 1650)(Bucheli and Gustafsson, 2000); (c) Sum of OC in soot, coal tar, and asphalt- and bitumen-like substances vs. $\log(\sum_{13}\text{PAH})$ (solid line indicates the regression of all points; dotted line indicates the regression of all points except residential soil (RS) and residential street dust (RSD); (d) Sum of OC in soot, coal tar, and asphalt- and bitumen-like substances vs. $\log(\sum_{13}\text{PAH})$ (soild line indicates the regression of HMW PAHs in all points except RSD and RS; dotted line indicates the regression of LMW PAHs in all points except RSD and RS.)

much improved (R^2 = 0.96) when residential soil and residential street dust are excluded (Figure 2.3c). The improved correlation likely results because residential sources of OC have large contributions from recent OM and much lower PAH concentrations, suggesting different PAH–OC dynamics than for commercial source materials. This modified correlation indicates that coal tar, asphalt, and soot particles are likely sources or carriers of PAHs in the watershed, and that PAH levels in the stream and lake are more affected by CMs from commercial land use areas (i.e., commercial soil, dust from sealed and unsealed parking lots) than residential areas.

Petrogenic PAHs are derived from natural OM and petroleum-based products and contain predominantly LMW PAHs (2-3-ring), whereas pyrolytic PAHs are produced during combustion (including pyrolysis) and contain predominantly HMW PAHs (4-6 ring). The 13 PAHs were divided into LMW and HMW PAHs and their logarithm values were plotted against the sum of OC in soot, coal tar, and asphalt- and bitumen-like substances, again excluding the residential soil and street dust samples. HMW PAHs and LMW PAHs both are significantly correlated with the sum of OC (R^2 = 0.96 and 0.95) (Figure 2.3d). Concentrations of HMW PAHs are higher than LMW PAHs in all samples, indicating that combustion sources (e.g., soot, coal tar, asphalt) dominate PAHs in all samples.

2.3.5 Distribution of PAHs

The distribution of PAHs among CMs was estimated using measured or literature values of PAH concentrations in CM particles and mass percentages of CMs determined from quantitative petrography and measured or literature values of CM density (see

Appendix A for details) (Figure 2.4). These estimates represent potential relative contributions because actual PAH loadings for each CM in each sample were not measured (Figure 2.4), and because literature values associated with different CMs result in estimated $\sum_{11}$PAH that exceed measured $\sum_{11}$PAH (data not shown). This is not surprising given that literature values typically are determined for relatively fresh CM particles, and particle weathering and transport reduce PAH concentrations over time. PAHs can also redistribute over time from more weakly to more strongly sorbing CMs.

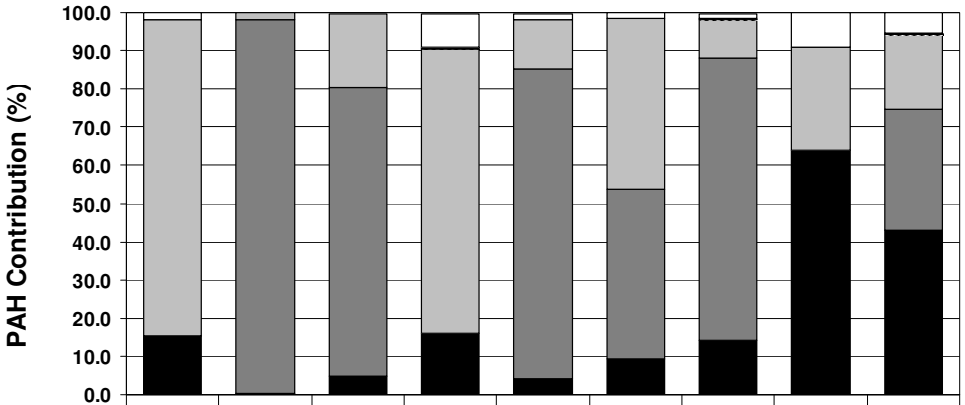

	RSD	SPD	UPD	RS	CS	IBS	LS 0-5	LS 10-15	LS 25-30
Recent OM	1.9	0.0	0.2	9.0	1.6	1.6	1.5	9.1	5.3
Hard Coal	0.0	0.0	0.0	0.3	0.1	0.0	0.1	0.0	0.3
Char	0.0	0.0	0.0	0.0	0.0	0.0	0.0	0.0	0.0
Coke	0.0	0.0	0.0	0.3	0.0	0.1	0.1	0.0	0.2
Asphalt- and Bitumen-like Substances	82.7	1.9	19.1	74.2	13.0	44.6	10.1	27.0	19.4
Coal-Tar Pitch	0.0	97.7	75.6	0.0	80.9	44.6	74.0	0.0	31.7
Soot	15.3	0.3	4.9	16.2	4.2	9.2	14.1	64.0	43.0

Figure 2.4. Distribution of PAHs among CMs in Lake Como watershed samples.

The estimated values suggest that the majority of PAHs in residential street dust and residential soil are associated with asphalt- and bitumen-like substances (83% and 74%, respectively). The majority of PAHs in sealed parking lot dust, unsealed parking lot dust, commercial soil, and top sediments are associated with coal-tar pitch (98%, 76%,

81%, and 74%, respectively). In streambed sediment, asphalt- and bitumen-like substances and coal-tar pitch play equally important roles, although the amount of asphalt- and bitumen-like substances is 25 times greater than the amount of coal-tar pitch. Soot dominates the distribution of PAHs in deeper lake sediments: 64% in sediments for the 10-15 cm depth and 43% for the 25-30 cm depth. The results suggest that coal-tar pitch, soot, and asphalt- and bitumen-like substances are important PAH sources in urban lake sediments. These results are consistent with the correlations between $\log(\sum_{13} \text{PAH})$ and OC in soot, coal-tar pitch, and asphalt- and bitumen-like substances discussed in the previous section.

2.3.6 PAH Loading from Coal-Tar Pitch

The mass of PAHs associated with coal-tar pitch in different samples was estimated to more directly explore its potential contribution to total PAH loadings. Results are shown in Figure 2.5. Recall that the measured value of the $\sum_{11} \text{PAH}$ concentration in coal-tar particles picked from the sealed parking lot sample was used. The estimated PAH loading contributed by coal-tar particles to 1 kg of sealed parking lot dust is 1,900 mg; this is not significantly different from the measured $\sum_{11} \text{PAH}$ in this sample. Given that greater than 97% of the total PAHs in this sample are from coal tar (Figure 2.4), this agreement indicates that parameter inputs used in our estimation were adequately determined for this sample. Extending the coal-tar loading results to other samples, the potential PAH loadings from coal tar are greater than the measured $\sum_{11} \text{PAH}$ in all samples where coal-tar particles were detected. These

differences are expected because PAH concentrations associated with coal-tar particles will decrease during runoff, during transport and deposition in surface water bodies, and in sediments after burial as a result of several processes, including volatilization, solubilization, degradation, and mass transfer to other CMs. Nevertheless, the results suggest that coal-tar particles are an important source of PAHs in urban lake sediments.

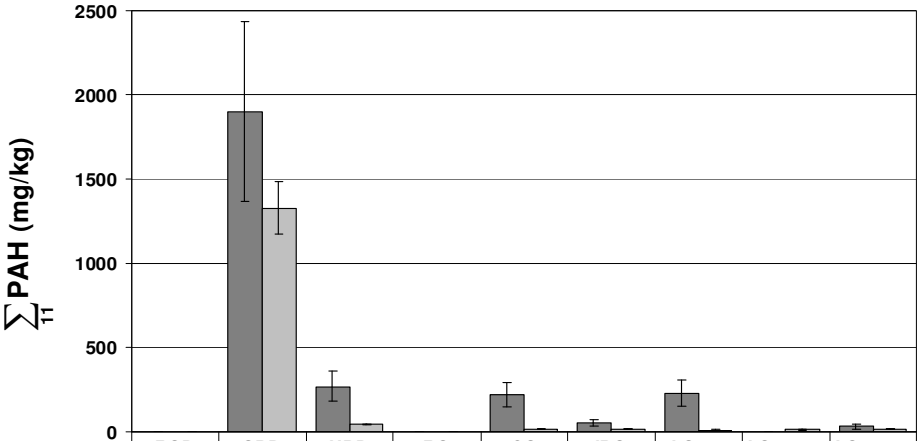

	RSD	SPD	UPD	RS	CS	IBS	LS 0-5	LS 10-15	LS 25-30
Potential Contribution from Coal Tar	0	1900	270	0	220	54	230	0	31
Measured Concentration	0.84	1330	44	0.72	16	15	9.5	11	15

Figure 2.5. Comparison between potential PAH loadings from coal-tar pitch and measured total PAHs in Lake Como watershed samples ($\sum_{11}$PAH as used here is the sum of 11 PAHs: phenanthrene, anthracene, fluoranthene, pyrene, benz(a)anthracene, chrysene, benzo[b]fluoranthene, benzo[k]fluoranthene, benzo(a)pyrene, indeno[1,2,3-cd]pyrene, and benzo[ghi]perylene. Error bars represent the precision of estimation or measurement. For estimated potential PAH loadings from coal tar pitch, it is ±1 standard deviation. For measured total PAHs in samples, it is absolute variation).

It is reasonable to infer from these estimates and the correlations between CMs and PAHs (Figure 2.3) that coal-tar pitch, asphalt, and soot are the primary sources and carriers of PAHs in our studied watershed. Several decades of research on urban sources of PAHs mainly focused on automobile exhaust, lubricating oils, gasoline, tire particles, asphalt and bitumen, and atmospheric deposition (Wakeham et al., 1980; Takada et al.,

1990; Simcik et al., 1996; Brandt and De Groot, 2001; Pengchai et al., 2004). Only recently has use of coal-tar sealants been identified as an important urban source of PAHs (Mahler et al., 2005). Because of the high intrinsic PAH levels in coal tar and the widespread and repeated application of coal-tar sealants on impervious surfaces, the abrasion of sealant likely generates a significant amount of coal-tar particles that contribute to PAH contamination in urban settings (Van Metre et al., 2009). Lacking specific knowledge of how coal-tar particles influence the transport and fate of PAHs in urban watersheds makes it difficult to make informed management decisions. For example, if coal-tar pitch is an important source of PAHs in urban lake sediments, stormwater management strategies that rely on trapping relatively coarse sediments might be ineffective. Thus improving understanding of the relations between PAHs with CM particles in urban runoff should assist in stormwater management and policy decision.

2.4 References

Ahn, S., D. Werner, R.G. Luthy, 2005, Physicochemical characterization of coke-plant soil for the assessment of polycyclic aromatic hydrocarbon availability and the feasibility of phytoremediation, Environmental Toxicology And Chemistry, 24(9), 2185-2195.

Boonyatumanond, R., M. Murakami, G. Wattayakorn, A. Togo, H. Takada, 2007, Sources of polycyclic aromatic hydrocarbons (PAHs) in street dust in a tropical Asian mega-city, Bangkok, Thailand, Science Of The Total Environment, 384(1-3), 420-432.

Brandt, H.C.A., P.C. De Groot, 2001, Aqueous leaching of polycyclic aromatic hydrocarbons from bitumen and asphalt, Water Research, 35(17), 4200-4207.

Breedveld, G.D., E. Pelletier, R. St Louis, G. Cornelissen, 2007, Sorption characteristics of polycyclic aromatic hydrocarbons in aluminum smelter residues, Environmental Science & Technology, 41(7), 2542-2547.

Bucheli, T. D., O. Gustafsson, 2000, Quantification of the soot-water distribution coefficient of PAHs provides mechanistic basis for enhanced sorption observations, Environmental Science & Technology, 34(24), 5144-5151.

Chalmers, A.T., P.C. Van Metre, E. Callender, 2007, The chemical response of particle-associated contaminants in aquatic sediments to urbanization in New England, USA, Journal of Contaminant Hydrology, 91(1-2), 4-25.

Ghosh, U., J.R. Zimmerman, R.G. Luthy, 2003, PCB and PAH speciation among particle types in contaminated harbor sediments and effects on PAH bioavailability, Environmental Science & Technology, 37(10), 2209-2217.

Gustafsson, O., F. Haghseta, C. Chan, J. MacFarlane, P.M. Gschwend, 1997, Quantification of the dilute sedimentary soot phase: Implications for PAH speciation and bioavailability, Environmental Science & Technology, 31(1), 203-209.

Heiri, O., A.F. Lotter, G. Lemcke, 2001, Loss on ignition as a method for estimating organic and carbonate content in sediments: reproducibility and comparability of results, Journal of Paleolimnology, 25(1), 101-110.

Horowitz, A.J., K.A. Elrick, 1987, The relation of stream sediment surface area, grain size and composition to trace element chemistry, Applied Geochemistry, 2(4), 437-451.

Jeong, S., M.M. Wander, S. Kleineidam, P. Grathwohl, B. Ligouis, C. J. Werth, 2008, The role of condensed carbonaceous materials on the sorption of hydrophobic organic contaminants in subsurface sediments, Environmental Science & Technology, 42(5), 1458-1464.

Jonker, M.T.O., S.B. Hawthorne, A.A. Koelmans, 2005, Extremely slowly desorbing polycyclic aromatic hydrocarbons from soot and soot-like materials: Evidence by supercritical fluid extraction, Environmental Science & Technology, 39(20), 7889-7895.

Karapanagioti, H.K., S. Kleineidam, D.A. Sabatini, P. Grathwohl, B. Ligouis, 2000, Impacts of heterogeneous organic matter on phenanthrene sorption: Equilibrium and kinetic studies with aquifer material, Environmental Science & Technology, 34(3), 406-414.

Khalil, M.F., U. Ghosh, J.P. Kreitinger, 2006, Role of weathered coal tar pitch in the partitioning of polycyclic aromatic hydrocarbons in manufactured gas plant site sediments, Environmental Science & Technology, 40(18), 5681-5687.

Khalili, N.R., P.A. Scheff, T.M. Holsen, 1995, PAH source fingerprints for coke ovens, diesel and gasoline-engines, highway tunnels, and wood combustion emissions, Atmospheric Environment, 29(4), 533-542.

Kimbrough, K.L., R.M. Dickhut, 2006, Assessment of polycyclic aromatic hydrocarbon input to urban wetlands in relation to adjacent land use, Marine Pollution Bulletin, 52(11), 1355-1363.

MacDonald, D.D., C.G. Ingersoll, T.A. Berger, 2000, Development and evaluation of consensus-based sediment quality guidelines for freshwater ecosystems, Archives of Environmental Contamination and Toxicology, 39(1), 20-31.

Mahler, B.J., P.C. Van Metre, 2003, A simplified approach for monitoring hydrophobic organic contaminants associated with suspended sediment: Methodology and applications, Archives Of Environmental Contamination And Toxicology, 44(3), 288-297.

Mahler, B.J., P.C. Van Metre, T.J. Bashara, J.T. Wilson, D.A. Johns, 2005, Parking lot sealcoat: An unrecognized source of urban polycyclic aromatic hydrocarbons, Environmental Science & Technology, 39(15), 5560-5566.

Motelay-Massei, A., B. Garban, K. Tiphagne-larcher, M. Chevreuil, D. Ollivon, 2006, Mass balance for polycyclic aromatic hydrocarbons in the urban watershed of Le Havre (France): Transport and fate of PAHs from the atmosphere to the outlet, Water Research, 40(10), 1995-2006.

Murakami, M., F. Nakajima, H. Furumai, 2005, Size- and density-distributions and sources of polycyclic aromatic hydrocarbons in urban road dust, Chemosphere, 61(6), 783-791.

Murakami, M., J. Yamada, H. Kumata, H. Takada, 2008, Sorptive behavior of nitro-PAHs in street runoff and their potential as indicators of diesel vehicle exhaust particles, Environmental Science & Technology, 42(4), 1144-1150.

Olson, M.C., J.L. Iverson, E.T. Furlong, M.P. Schroeder, 2003, Methods of analysis by the U.S. Geological Survey National Water Quality Laboratory—Determination of polycyclic aromatic hydrocarbon compounds in sediment by gas chromatography/mass spectrometry, U.S. Geological Survey Water-Resources Investigations Report 03-4318, Denver, CO, U.S. Geological Survey**,** 45pp.

Pengchai, P., H. Furumai, F. Nakajima, 2004, Source apportionment of polycyclic aromatic hydrocarbons in road dust in Tokyo, Polycyclic Aromatic Compounds, 24(4-5), 773-789.

Rogge, W.F., L.M. Hildemann, M.A. Mazurek, G.R. Cass, B.R.T. Simoneit, 1993a, Sources of fine organic aerosol .2. Noncatalyst and catalyst-equipped automobiles and heavy-duty diesel trucks, Environmental Science & Technology, 27(4), 636-651.

Rogge, W.F., L.M. Hildemann, M.A. Mazurek, G.R. Cass, B.R.T. Simoneit, 1993b, Sources of fine organic aerosol. 3. Road dust, tire debris, and organometallic brake lining

dust: Roads as sources and sinks, Environmental Science & Technology, 27(9), 1892-1904.

Rogge, W.F., L.M. Hildemann, M.A. Mazurek, G.R. Cass, B.R.T. Simoneit, 1997, Sources of fine organic aerosol .7. Hot asphalt roofing tar pot fumes, Environmental Science & Technology, 31(10), 2726-2730.

Rogge, W.F., L.M. Hildemann, M.A. Mazurek, G.R. Cass, B.R.T. Simoneit, 1998, Sources of fine organic aerosol. 9. Pine, oak and synthetic log combustion in residential fireplaces, Environmental Science & Technology, 32(1), 13-22.

Scoggins, M., N.L. McClintock, L. Gosselink, P. Bryer, 2007, Occurrence of polycyclic aromatic hydrocarbons below coal-tar-sealed parking lots and effects on stream benthic macroinvertebrate communities, J. N. Am. Benthol. Soc., 26(4), 694-707.

Simcik, M.F., S.J. Eisenreich, K.A. Golden, S.P. Liu, E. Lipiatou, D.L. Swackhamer, D.T. Long, 1996, Atmospheric loading of polycyclic aromatic hydrocarbons to Lake Michigan as recorded in the sediments, Environ. Sci. Technol., 30(10), 3039-3046.

Takada, H., T. Onda, N. Ogura, 1990, Determination of polycyclic aromatic hydrocarbons in urban street dusts and their source materials by capillary gas-chromatography, Environmental Science & Technology, 24(8), 1179-1186.

Taylor, G.H., M. Teichmuller, A. Davis, C.F.K. Diessel, R. Littke, P. Robert, 1998, *Organic Petrology*, Berlin, Gebrüder Borntraeger.

Tsapakis, M., E.G. Stephanou, I. Karakassis, 2003, Evaluation of atmospheric transport as a nonpoint source of polycyclic aromatic hydrocarbons in marine sediments of the Eastern Mediterranean, Marine Chemistry, 80(4), 283-298.

Valle, S., M.A. Panero, L. Shor, 2007, Pollution Prevention and Management Strategies for Polycyclic Aromatic Hydrocarbons in the New York/New Jersey Harbor. Harbor Consortium of the New York Academy of Sciences. New York**:** 170 pp.

Van Metre, P.C., B.J. Mahler, 2004, Contaminant trends in reservoir sediment cores as records of influent stream quality, Environmental Science & Technology, 38(11), 2978-2986.

Van Metre, P.C., B.J. Mahler, 2005, Trends in hydrophobic organic contaminants in urban and reference lake sediments across the United States, 1970-2001, Environmental Science & Technology, 39(15), 5567-5574.

Van Metre, P.C., B.J. Mahler, J.T. Wilson, 2009, PAHs underfoot: Contaminated dust from coal-tar sealcoated pavement is widespread in the United States, Environmental Science & Technology, 43(1), 20-25.

Van Metre, P.C., J.T. Wilson, G.R. Harwell, M.O. Gary, F.T. Heitmuller, B.J. Mahler, 2003, Occurrence, trends, and sources in particle-associated contaminants in selected streams and lakes in Fort Worth, Texas. USGS Water-Resources Investigations Report 03–4169, Denver, CO, U.S. Geological Survey**,** 66 pp.

Wakeham, S.G., C. Schaffner, W. Giger, 1980, Polycyclic Aromatic-Hydrocarbons In Recent Lake-Sediments .1. Compounds Having Anthropogenic Origins, Geochimica Et Cosmochimica Acta, 44(3), 403-413.

Wilson, J.T., P.C. Van Metre, C.J. Werth, Y. Yang, 2006, Particle-associated contaminants in street dust, parking lot dust, soil, lake- bottom sediment, and suspended and streambed sediment, Lake Como and Fosdic Lake watersheds, Fort Worth, Texas, 2004 U.S. Geological Survey Data Series 211. Denver, CO, U.S. Geological Survey http://pubs.usgs.gov/ds/2006/211/ (accessed May 2009)**,** 24pp.

Zhang, J., L.Z. Cai, D.X. Yuan, M. Chen, 2004, Distribution and sources of polynuclear aromatic hydrocarbons in Mangrove surficial sediments of Deep Bay, China, Marine Pollution Bulletin, 49(5-6), 479-486.

Chapter 3

Potential Contributions of Asphalt and Coal Tar to Black Carbon Quantification in Urban Dust, Soils, and Sediments

3.1. Introduction

Black carbon (BC) is a particulate carbonaceous material (CM) produced from the incomplete combustion of fossil fuel and biomass (Goldberg, 1985). It is ubiquitous in soil, sediment, water, and the atmosphere, and is involved in many biogeochemical and environmental processes (Kuhlbusch, 1998; Schmidt and Noack, 2000; Forbes et al., 2006). BC sequestered in soils and sediments plays an important role as a sink of carbon (C) in the global C cycle because of its stability in the environment (Gustafsson and Gschwend, 1998; Kuhlbusch, 1998; Masiello and Druffel, 1998). Because of its strong sorption properties, BC sequestered in soils and sediments also affects the transport and fate of persistent organic pollutants (POPs) in aquatic environments, such as polychlorinated biphenyls (PCBs) (Jonker and Smedes, 2000; Jonker and Koelmans, 2002) and polycyclic aromatic hydrocarbons (PAHs) (Cornelissen et al., 2005; Jonker and Koelmans, 2002).

Although petrogenic sources of BC (weathering of graphite from rocks) have been reported in marine sediments (Dickens et al., 2004), BC is usually pyrogenic in origin, and spans a continuum of materials ranging from slightly charred biomass to highly refractory soot (Elmquist et al., 2006; Hedges et al., 2000; Masiello, 2004). The BC continuum is often broadly separated into two groups, char-BC and soot-BC, which

have different physicochemical properties. Char-BC is charred organic residues (e.g., wood char) formed at lower temperatures, and retains some morphological features of the precursors (Nguyen et al., 2004). Soot-BC is the condensed vapor phase of combustion and consists of a more randomly ordered inner core and a more crystallized outer shell (Gustafsson et al., 2001). The formation mechanisms of char- and soot-BC cause them to be more recalcitrant than other biologically or geologically-generated CMs, such as humic substances, coal, and kerogen.

Current methods to quantify BC in soils and sediments include quantitative petrography (Cornelissen et al., 2004), acid dichromate oxidation (Gelinas et al., 2001; Jeong et al., 2008; Lim and Cachier, 1996; Masiello and Druffel, 1998; Masiello et al., 2002; Song et al., 2002), and chemo-thermal oxidation at 375ºC (CTO-375) (Elmquist et al., 2004; Gustafsson et al., 2001; Gustafsson and Gschwend, 1997; Gustafsson et al., 1997; Nguyen et al., 2004). The first of these methods requires particles larger than the wavelength of light, and employs fluorescent and phase contrast microscopy. The latter two of these methods rely on the chemical and thermal stability of BC. They involve removing minerals and non-BC CM components using chemical treatments and/or thermal oxidation, followed by elemental analysis. Because of the complexity of natural matrices, and the existence of potential interfering materials, BC contents in soils and sediments determined by different techniques can vary widely (Hammes et al., 2007; Schmidt et al., 2001). Some non-pyrogenic CMs, such as melanoidin, kerogen, lignite coal, and bituminous coal, have been suggested to result in overestimation of BC in soil and sediment samples because these materials are either chemically recalcitrant or

charred during heating (Brodowski et al., 2005; Gustafsson et al., 2001; Hammes et al., 2007).

In urban watersheds, asphalt and coal tar particles worn from infrastructure surfaces (pavements and roofs) can be present in soils, stream and lake sediments, and their effect on BC quantification has heretofore not been explored. Asphalt (in this study) is the dark brown to black cementitious material that remains after the distillation of crude oil and commonly used as a paving material. The words bitumen and asphaltic bitumen have been used instead of asphalt in countries other than the United States (Zakar, 1971). Coal tar is a black sticky substance that remains after coal carbonization or gasification. It is widely used as a binding material in the aluminum and graphite industries, and as a primary ingredient of sealcoats used in pavement and building applications. Asphalt and coal-tar-based sealcoats undergo weathering and break into particles as a result of vehicle traffic, exposure to sunlight and air, and freeze-thaw cycles (Freemantle, 1999; Mahler et al., 2005). Runoff can carry particles into soils, streams, and lakes. The pyrogenic origins of asphalt and coal tar suggest they may be resistant to chemical and thermal treatment used for BC quantification.

The primary objectives of this study are to explore the effects of asphalt and coal tar on the quantification of BC in a range of urban environmental samples, and to evaluate biases in the different methods used for quantifying BC. Samples evaluated were reference asphalt and coal-tar materials, as well as pavement dust, residential and commercial soil, and lake sediments from a small urban watershed. Total BC was quantified using a series of chemical treatments that includes Cr_2O_7 oxidation, and CTO-375. BC species including soot and char/charcoal, asphalt, and coal tar were quantified

using petrographic analysis. This approach allows us to test the hypothesis that both asphalt and coal tar are resistant to oxidation using Cr_2O_7 or CTO-375, and therefore contribute to BC amounts determined with these methods.

3.2 Materials and Methods

3.2.1 Sample Collection, Preparation, and C Analysis

Field samples (pavement dust, soils, and lake sediments) from Lake Como watershed, Fort Worth, Texas, asphalt and coal-tar particles picked from representative field samples, and reference asphalt binder and coal-tar sealcoat were used in this study. Details of the Lake Como sampling site and sample collection methods were described in Chapter 2. Briefly, one composite residential street dust sample was collected from three asphalt-paved residential streets using nylon push brooms and stainless steel dust pans. Two composite parking lot dust samples were collected; one was a composite of dust from three coal-tar-sealed commercial parking lots and the other was a composite of dust from three unsealed asphalt or cement commercial parking lots. Two composite surface soil samples (top 2 cm) were collected randomly at approximately 40 locations near roads, sidewalks and driveways using stainless steel scoops; one was from a residential neighborhood and the other was from a commercial area. Three sediment cores several meters apart were collected from a single site in Lake Como using a box corer. The cores were vertically extended and sliced at 5-cm intervals, and subsamples from the same depths (depth from the top: 0-5 cm, 10-15 cm, and 25-30 cm) were combined from the three cores to create three large-volume samples. Each composite sample was homogenized after passing through a 1-mm sieve.

Particles of asphalt and coal tar were physically separated from unsealed parking lot dust and sealed parking lot dust, respectively, after treatment with hydrochloric and hydrofluoric acid (HCl/HF) to remove carbonate and silicate minerals and enrich in C. The target particles were identified in bulk samples with a Leitz DMRX-MPVSP photometer microscope using reflected white light and UV+violet-light illumination (fluorescence mode). The particles were then picked from the bulk samples using tweezers. The reference asphalt binder was obtained from Frontier Refining, Inc., in Cheyenne, WY. The reference coal tar was obtained by evaporating the liquid component of a coal-tar-based emulsion driveway sealcoat, obtained from Henry Company, El Segundo, CA.

The C contents of all bulk samples were determined with a CE 440 CHN analyzer (Exeter Analytical, Inc., North Chelmsford, MA) in the Microanalysis Laboratory at the University of Illinois at Urbana-Champaign (UIUC), after the removal of inorganic C with 5% H_2SO_3 followed by oven drying, and is referred to as total organic C (TOC). The TOC includes both non-BC organic carbon (OC) and BC.

3.2.2 Density Separation

Representative sub-samples of Lake Como watershed field samples were separated into light (LFr) and heavy (HFr) fractions with a solution of 1.60 g/cm^3 sodium polytungstate. Both fractions were oven dried at 60ºC, pulverized, and passed through a 100-mesh sieve to enhance reaction kinetics of subsequent chemical and thermal treatments.

3.2.3 C_2O_7 Oxidation

Both HFr and LFr fractions were subject to a series of chemical treatment steps to obtain fractions enriched in one or more particulate CMs. Procedures were the same as described in Jeong et al. (Jeong et al., 2008; Jeong and Werth, 2005). Briefly, samples were treated sequentially with HCl, HF/HCl, trifluoroacetic acid (TFA)/HCl, sodium hydroxide (NaOH), and acid dichromate ($K_2Cr_2O_7/H_2SO_4$) to remove carbonates, silicate minerals (Durand, 1980), easily hydrolyzable organic matter (Gelinas et al., 2001), fulvic and humic acids (Swift, 1996), and more recalcitrant humin and kerogen (Lim and Cachier, 1996; Masiello et al., 2002), respectively. Mass fractions of different CM enrichments were obtained by measuring changes of sample mass after each treatment step, and the final residues (i.e., after $K_2Cr_2O_7/H_2SO_4$) are referred to as BC fractions. More than three replicate HFr fractions were sequentially treated through $K_2Cr_2O_7/H_2SO_4$, hereafter referred to as Cr_2O_7 treatment. Only one sample of each LFr fraction was treated in this way due to sample mass limitations. The C and hydrogen (H) contents of LFr and HFr fractions after the removal of inorganic C, and their BC enrichment fractions, were determined using a CHN analyzer. The final C in BC enrichment fractions is referred to as BC determined by Cr_2O_7 oxidation. The BC contents in both fractions are expressed as gram BC per kilogram of bulk samples (g/kg) in the results.

The same sequential chemical treatment was also applied to the reference asphalt and coal tar samples. To enhance the reaction rates, fine particles of coal tar, or coal tar and asphalt coated on inert supporting materials, were used. Support materials inert to all chemicals used during treatment were not identified. As a result, pyrite (WARD'S Natural Science, Rochester, NY) was used as the support material for treatment with HCl

and HF/HCl because it is resistant to these two acids but not dichromate, and glass was used as the support material for treatment with TFA/HCl, NaOH, and $K_2Cr_2O_7/H_2SO_4$, because it is resistant to strong oxidants but not HF. Dried coal tar was cut into < 1 mm pieces and asphalt was coated on fine pyrite particles (< 1 mm) before use in HCl and HF/HCl treatment. A control with pyrite particles was also performed. Asphalt and coal tar were coated on glass slides (2 cm by 2 cm) in thin layers (< 1 mm) for subsequent chemical treatment steps. Changes in sample mass after each treatment step were recorded. The final remaining mass percentage was determined by the combination of remaining mass percentages after each step of chemical treatment. The C and H contents of original samples after the removal of inorganic C and the residues after the final Cr_2O_7 oxidation were measured by CHN analysis. Chemical treatment through Cr_2O_7 was not applied to asphalt and coal-tar particles separated from the Lake Como unsealed and sealed parking lot samples, respectively, due to the limited mass of these samples.

3.2.4 Thermal Treatment (CTO-375)

BC contents in bulk samples and LFr and HFr fractions were determined in triplicate by a modified CTO-375 method (Gustafsson and Gschwend, 1997). About 20-50 mg of well-pulverized samples (< 150 μm) were combusted in a Thermolyne F62700 muffle furnace (Barnstead International, Dubuque, IA) in excess air at 375 °C for 24 h, followed by carbonate removal with 1M HCl, and the C and H contents of the remaining mass were determined by CHN analysis. The measured C contents after CTO-375 and HCl treatment are the BC contents. BC contents in reference asphalt and coal tar materials, and in separated asphalt and coal-tar particles from the Lake Como samples, were also estimated with CTO-375.

3.2.5 Organic Petrography

Petrographic methods and results were reported in Chapter 2, and are presented in this chapter for comparison. Quantitative organic petrographic analysis was performed after the removal of carbonate and silicate minerals with HCl/HF. Sample preparation involved embedding CM-enriched samples on the surface of epoxy resin, allowing the resin to cure and harden, and then polishing the sample surface. Embedded samples were observed with a Leitz DMRX-MPVSP photometer microscope using reflected white light and UV+violet-light illumination (fluorescence mode). CM particles were identified and classified according to maceral groups and their subgroups defined by Taylor et al. (1998). Volume fractions of macerals in each sample were determined by point counting of at least 500 macerals using a multi-point cross-hair ocular. The overall accuracy has been determined to be approximately ±2% (Taylor et al., 1998).

The contributions of different CMs to the TOC of each sample were estimated with volume fractions of CMs determined by organic petrography, densities and OC contents of CMs determined from the literature or in our laboratory, and TOC of bulk samples. The corresponding equations for this calculation and sources of density and OC contents are shown in Appendices A and B (Table A1, A2, and B1).

The BC contents of CMs identified with petrography were determined by multiplying OC contributions by BC to OC ratios (BC/OC) obtained from the literature or measured in our laboratory. For soot, a literature value of BC/OC (0.63) was obtained from the average BC contents after CTO-375 of several reference materials, including diesel soot SRM-2975, diesel soot SRM-1650, and n-hexane soot (Elmquist et al., 2006). For asphalt and coal tar, BC/OC ratios were measured for reference materials using both

Cr_2O_7 oxidation and CTO-375. Values from Cr_2O_7 oxidation were used when comparing BC from this method with BC from petrography, and values from CTO-375 were used when comparing BC from this method to BC from petrography. Char was not present in sufficient quantities to justify calculating BC quantities, and other CMs do not directly contribute to BC contents.

3.3 Results and Discussion

3.3.1 BC Determined by Cr_2O_7 Oxidation

The TOC contents of bulk samples, mass percentages of LFr and HFr fractions, and the distribution of OC and BC between LFr and HFr fractions are shown in Table 3.1. Recall that OC includes both non-BC and BC fractions of C after treatment to remove inorganic C. The majority of mass is associated with HFr fractions in all samples (97.1-99.7%), so are the OC and BC. The OC contents range from 14.8 g/kg to 49.6 g/kg in HFr fractions, and from 0.8 g/kg to 8.6 g/kg in LFr fractions. The dominance of HFr-associated OC over LFr-associated OC is greater in the sediments (~98%) than in the soils and dust (63-90%). The discrepancies (ranging from 0.1 to 25%) between measured TOCs of bulk samples and the sum of OC in LFr and HFr samples is attributed to the loss of water soluble OC during density separation.

Table 3.1. Measured TOC in bulk samples, the mass percentages of LFr and HFr fractions, the distribution of OC and BC between LFr and HFr fractions, and the ratios of H/C in BC determined by Cr_2O_7 oxidation.

Sample ID		RSD	SPD	UPD	RS	CS	LS 0-5	LS 10-15	LS 25-30
TOC (g/kg) [a]		28.7±1.8	42.0±2.9	27.8±2.5	28.0±1.3	40.0±0.7	39.2±0.6	47.1±2.3	50.4±1.4
Mass (%)	**LFr**	2.22±0.10[b]	2.09±0.12	1.91±0.08	0.88±0.08	2.25±0.13	0.36±0.02	0.32±0.02	0.30±0.02
	HFr	97.07±0.46	97.68±0.12	97.47±0.36	98.82±0.30	97.71±0.18	99.64±0.03	99.68±0.03	99.71±0.03
OC (g/kg)	**LFr**	8.57	8.31	6.57	2.26	7.00	0.95	0.76	0.78
	HFr	14.83	35.56	15.10	20.76	31.27	35.40	41.16	49.55
	Sum	23.4	43.87	21.67	23.02	38.27	36.35	41.92	50.33
Contribution to OC (%)	**LFr**	36.63	18.94	30.31	9.84	18.28	2.60	1.81	1.55
	HFr	63.37	81.06	69.69	90.16	81.72	97.40	98.19	98.45
BC (g/kg)	**LFr**	1.38	2.97	0.75	0.26	0.44	0.14	0.17	0.19
	HFr	4.87	13.82	4.18	3.49	2.59	9.99	11.11	11.51
	Sum	6.25	16.79	4.93	3.75	3.03	10.13	11.28	11.70
Contribution to BC (%)	**LFr**	22.08	17.68	15.27	6.88	14.41	1.42	1.50	1.61
	HFr	77.92	82.32	84.73	93.12	85.59	98.58	98.50	98.39
H/C in BC	**LFr**	0.11	0.06	0.09	0.11	0.11	0.10	0.10	0.10
	HFr	0.12	0.07	0.12	0.11	0.10	0.11	0.12	0.12

a. Original data was presented in Chapter 2
b. Represents averages and standard deviations of replicates ≥3

Similar to OC, the majority of BC is associated with HFr fractions in all samples, and the dominance of HFr-associated BC over LFr-associated BC is greater in the sediments (> 98%) than in the soils and dust (78-93%). Sealed parking lot dust has the largest amount of total BC (16.8 g/kg), followed by sediment samples (11.7, 11.3, and 10.1 g/kg for depths of 25-30cm, 10-15cm, 0-5 cm, respectively), residential street dust (6.3 g/kg), unsealed parking lot dust (4.9 g/kg), residential soil (3.8 g/kg), and commercial soil (3.0 g/kg). H/C ratios of BC in LFr and HFr fractions separated by Cr_2O_7 oxidation are between 0.06 and 0.1 (Table 3.1), within the range of reported values determined by Cr_2O_7 oxidation for the BC continuum, especially for char-BC and soot-BC (0-0.6 by Hammes et al. (2007) and 0-0.8 by Kuo et al. (2008)).

Mass loss of reference asphalt and coal tar materials after each step of chemical treatment is presented in Figure B1 (Appendix B). Approximately 90% of the original asphalt mass remains after Cr_2O_7 oxidation; ~3% is lost after HCl/HF demineralization, ~6% after TFA and NaOH extraction, and ~1% after Cr_2O_7 oxidation. Approximately 46% of the original coal tar mass remains after Cr_2O_7 oxidation; ~15% is lost after HCl/HF demineralization, ~37% after TFA and NaOH extraction, and ~2% after Cr_2O_7 oxidation. CHN analysis indicates that BC in Cr_2O_7-oxidized asphalt residue (referred to as asphalt-BC) is 727 g/kg of asphalt, and BC in Cr_2O_7-oxidized coal-tar residue (referred to as coal-tar-BC) is 245 g/kg of coal tar. H/C ratios of asphalt and coal tar residues are 0.1 and 0.05, within the aforementioned range for BC continuum (Hammes et al., 2007; Kuo et al., 2008) (Table B2 in Appendix B).

3.3.2 BC Determined by CTO-375

The BC contents in LFr and HFr fractions determined by CTO-375 are presented in Table 3.2. The amounts of BC detected by CTO-375 are consistently lower than those detected by Cr_2O_7 oxidation in the same samples; however, some trends are similar. The majority of BC is associated with HFr fractions in all samples (> 98% in the sediments, and 69-95% in the soils and dust). Sealed parking lot dust has the largest amount of BC in bulk samples (3.0 g/kg), followed by sediment samples (2.4, 2.1, and and 2.1 g/kg for depths of 25-30cm, 10-15cm, 0-5 cm, respectively), soils (1.5 g/kg for commercial soil and 1.1 g/kg for residential soil), and dust (1.0 g/kg for unsealed parking lot dust and 0.9 for residential street dust). The differences between the sum of BC in LFr and HFr fractions and BC determined in bulk samples (5 to 39% difference) is due to experimental errors and loss of BC during density separation. The H/C ratios of BC in bulk samples determined by CTO-375 are between 0.1 and 0.4 (Table 3.2), also within the range of reported values determined by CTO-375 for the BC continuum, especially for char-BC and soot-BC (0-0.6 by Hammes et al. (2007)).

BC determined by CTO-375 in the commercial coal tar product is 71.8 g/kg coal tar, similar to that in separated coal tar particles (69.2 g/kg coal tar) (Table B2).When combusted at 375 ºC with air for 24 h, commercial asphalt product had nearly no residue left; neither did separated asphalt particles, indicating that asphalt is not thermally recalcitrant. This result agrees with the previous report that pyrogenous asphalt undergoes thermal decomposition (depolymerization) when heated to a temperature above 300 ºC (Abraham 1960). The H/C ratio of coal-tar residues is 0.04 for the commercial product and 0.02 for the separated particles (Table B2).

Table 3.2. BC contents in bulk samples, the distribution of BC between LFr and HFr fractions, and the ratios of H/C in BC determined by CTO-375 method.

Sample ID		RSD	SPD	UPD	RS	CS	LS 0-5	LS 10-15	LS 25-30
BC (g/kg)	LFr	0.31	0.45	0.28	0.056	0.16	0.034	0.026	0.024
	HFr	1.03	1.75	0.61	1.16	1.00	1.80	2.23	1.77
	Sum	1.34	2.20	0.89	1.22	1.16	1.83	2.26	1.79
	Bulk	0.90	2.97	1.00	1.10	1.50	2.12	2.15	2.40
Contribution to BC (%)	LFr	23.02	20.44	31.01	4.64	13.77	1.82	1.16	1.32
	HFr	76.98	79.56	68.99	95.36	86.23	98.18	98.84	98.68
H/C in BC	Bulk	0.22	0.10	0.15	0.26	0.18	0.35	0.35	0.41

3.3.3 Char, Soot, Asphalt, and Coal Tar Determined by Organic Petrography

Two categories of CMs were identified by organic petrography: recent organic matter (OM) and anthropogenic CMs. Recent OM includes the following maceral groups: huminite, vitrinite, liptinite, and inertinite. CMs resulting from anthropogenic contamination include hard coal, coke, char, soot, and coal- and petroleum-derived fluorescent materials such as coal tar and asphalt which were referred to as coal-tar pitch and asphalt-like and bitumen-like substances in Chapter 2. The TOC of bulk samples estimated by summing OC contributed by all types of CMs identified with petrography (Table B1 in Appendix B) was compared with TOC measured by CHN analysis (Table 3.1); the results are presented in the Appendix B (Figure B2). The difference between the petrographic-TOC and CHN-TOC is between 25 % and 50%, indicating the magnitude of error in TOC for the range of samples evaluated using petrographic analysis.

Based on the measured TOC and the percentages of OC contributed by char, soot, asphalt, and coal tar, the OC contents of these CMs are presented in Figure 3.1. Char is often below the detection limit of organic petrography (0.2 vol % for particles greater than 1 to 2 microns) (Chapter 2). Its contribution to OC is negligible even though it was detected in some samples. Soot-OC and asphalt-OC were found in all samples. Soot-OC is higher in sediments (6.1-8.4 g/kg), but lower in soils and dust (1.0-3.5 g/kg). Asphalt-OC is higher in dust (14.2-16.0 g/kg), but lower in soils and sediments (2.9-6.9 g/kg). Coal-tar-OC dominates sealed parking lot dust (21.8 g/kg) and also exists in unsealed parking lot dust, commercial soil, and lake sediments for the depth of 0-5 and 25-30 cm (1.8, 1.3, 1.1, and 0.2 g/kg).

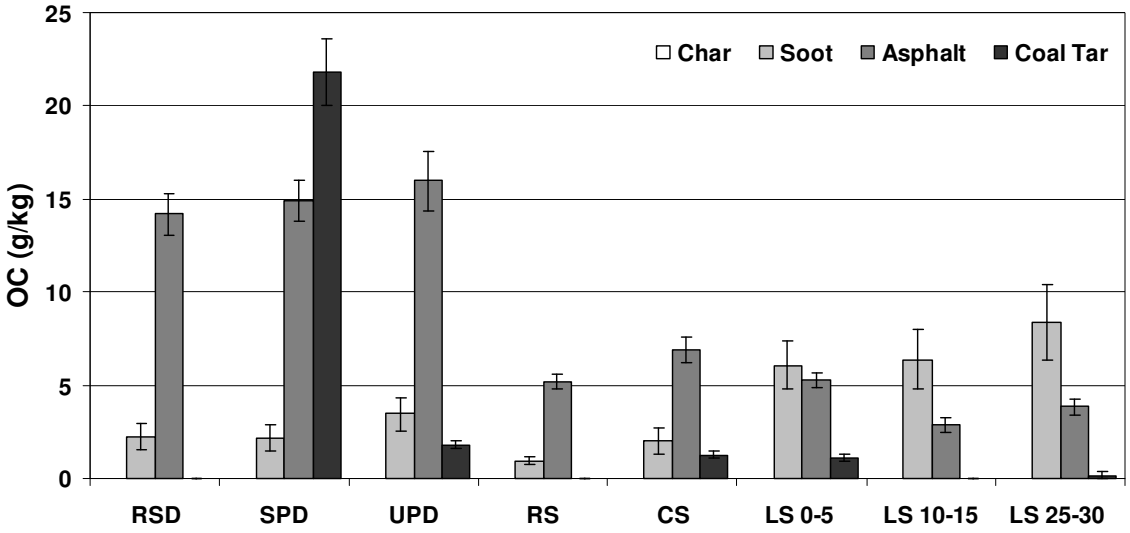

Figure 3.1. OC contributed by char, soot, asphalt, and coal tar in Lake Como watershed samples determined by organic petrography (samples include residential street dust (RSD), sealed parking lot dust (SPD), unsealed parking lot dust (UPD), residential soil (RS), commercial soil (CS), lake sediment from 0-5 cm depth (LS 0-5), lake sediment from 10-15 cm depth (LS 15-20), and lake sediment from 25-30 cm depth (LS 25-30) (Chapter 2).

3.3.4 Comparison of BC Quantified by Cr_2O_7 Oxidation, CTO-375, and Organic Petrography

BC contents quantified by Cr_2O_7 oxidation, CTO-375, and organic petrography are compared in Figure 3.2. The sum of BC in LFr and HFr fractions determined by Cr_2O_7 oxidation, BC in bulk samples determined by CTO-375, and soot-BC determined by organic petrography are compared (the amount of char-BC is negligible). Soot-BC determined by organic petrography and BC determined by CTO-375 are within a factor of 2 or statistically identical in several cases, but the amount of BC in samples quantified by Cr_2O_7 oxidation is 2-12 times greater than soot-BC quantified by organic petrography, and 2-7 times greater than BC quantified by CTO-375.

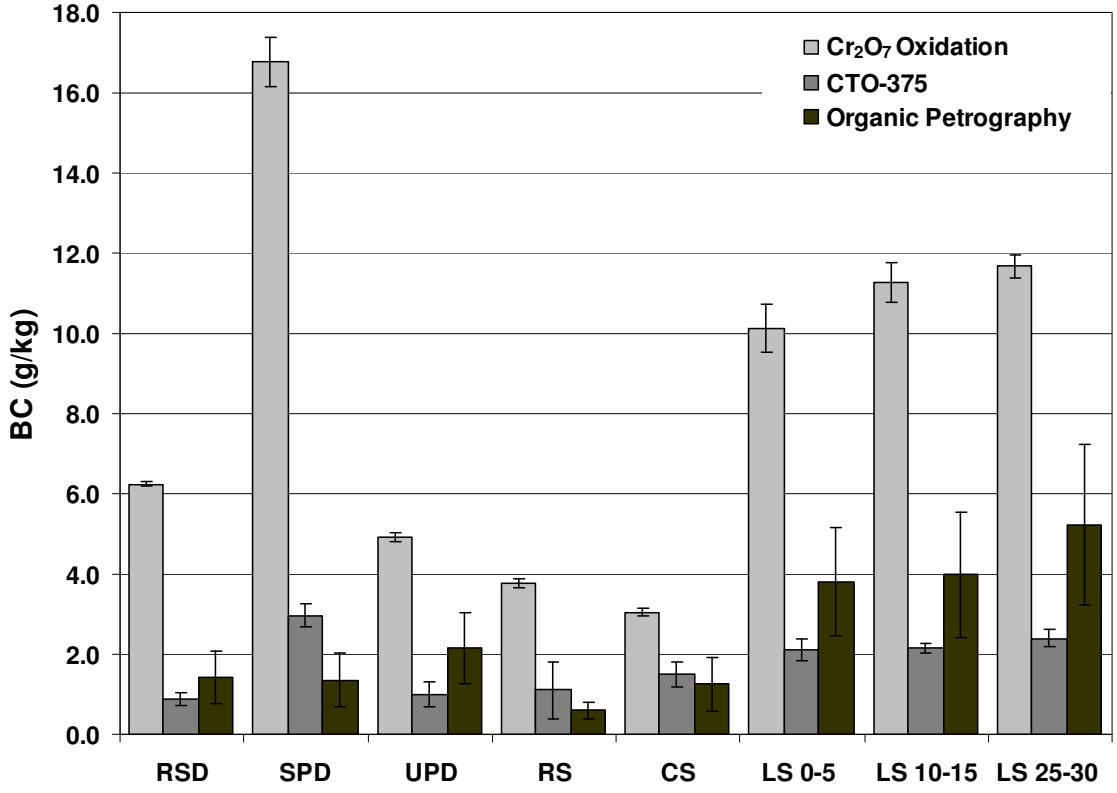

Figure 3.2. The comparison of BC in samples quantified by Cr_2O_7 oxidation, CTO-375, and. Soot-BC by organic petrography.

According to organic petrography, soot-BC contents are higher in the three lake sediment samples (3.8-5.2 g/kg) than in soil and dust samples (0.6-2.2 g/kg); however, sealed parking lot dust has the most abundant BC detected by Cr_2O_7 oxidation and CTO-375 methods, followed by sediments. The BC in sealed parking lot dust is 16.8 g/kg with Cr_2O_7 oxidation and 3.0 g/kg with CTO-375. The BC contents in sediments are 10.1-10.7 g/kg with Cr_2O_7 oxidation and 2.1-2.4 g/kg with CTO -375. Although these three quantification methods showed different patterns of BC distribution among different

types of samples (sediments, soils, and dust), they revealed a common trend that BC contents in sediments increase with depth of sediments, suggesting the accumulation of relatively more BC in sediments in past years, and the stability of BC in aquatic environment.

3.3.5 Contribution of Asphalt and Coal Tar to BC Determined by Cr_2O_7 Oxidation

The chemical treatment results of the reference asphalt and coal tar samples suggest that these materials likely contribute to high BC contents in samples determined with Cr_2O_7 oxidation. Hence, we included the contributions of BC by asphalt and coal tar with the contribution of soot in the petrographic results, and compared these values to the total BC determined by Cr_2O_7 oxidation in Figure 3.3. The BC contributed by asphalt and coal tar were calculated from the ratios of BC/OC in reference asphalt (0.86) and coal tar (0.39) materials (via Cr_2O_7 oxidation (Table B2)) and the OC contents contributed by asphalt and coal tar in each sample by petrography (Figure 3.1). The distribution patterns of total BC in pavement dust, soils, and sediments determined by these two methods are similar with greater amount of total BC in sealed parking lot dust than in other samples. Compared to the 2 – 12 times of difference between BC contents estimated by these two methods without considering the contribution of coal tar and asphalt (Figure 3.2), the difference after accounting for the contribution of coal tar and asphalt is within a factor of 2.5. Although OC contributed by coal tar in the sealed parking lot dust is higher than that contributed by asphalt, BC contributed by coal tar is lower than that contributed by asphalt in the same sample as a result of the higher BC/OC ratio of asphalt.

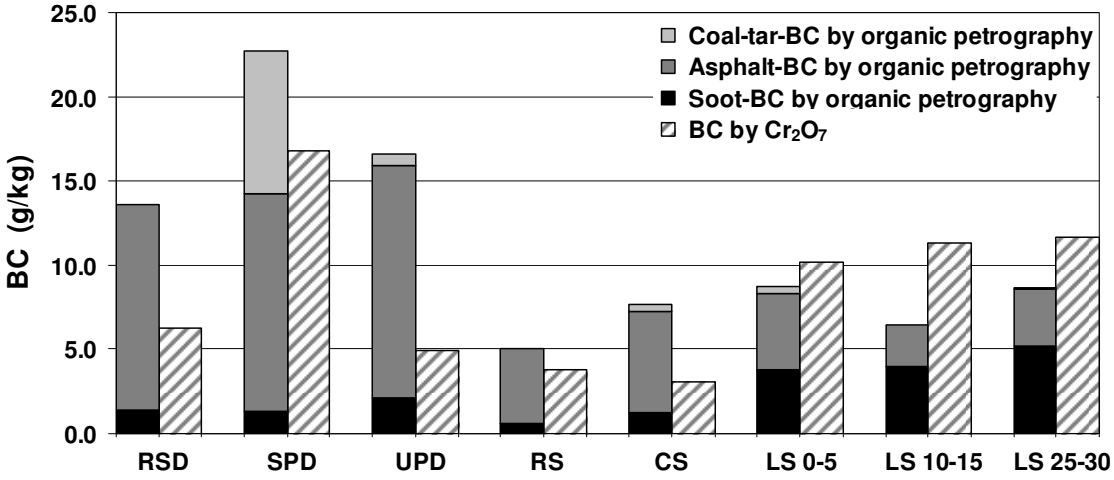

Figure 3.3. The comparison of BC quantified by Cr_2O_7 oxidation to the sum of soot-BC, asphalt-BC, and coal-tar-BC quantified by organic petrography.

Both asphalt and coal tar are mixtures of many organic compounds, and their chemical compositions and reactivity to chemicals depend on source materials (i.e. crude oil and coal) and production processes. Asphalt contains saturated and unsaturated aliphatic and aromatic compounds with up to 150 C atoms. Studies have showed that asphalt is highly resistant to chemical agents (including acids and bases) at ambient temperatures (Zakar, 1971). Coal tar are mixtures of hundreds of compounds composed of about two-thirds aromatic hydrocarbons and one-third of heterocyclic aromatic compounds (Chambrion et al., 1995). The estimated water solubility of coal tar is 16 mg/L (Peters and Luthy, 1993). Compared to coal tar, the oily composition of asphalt makes it less permeable to water (Zakar, 1971), reducing the penetration depth of aqueous phase chemicals; therefore, asphalt is more resistant to wet chemical oxidative treatment than coal tar, resulting in the higher measured BC/OC ratio. The stronger chemical recalcitrance of asphalt versus coal tar also partly explains the higher asphalt

contents in sediments determined by petrography, because chemical recalcitrance is more important for the stability of BC than thermal or physical recalcitrance (Liang et al., 2008).

The greatest difference between total BC determined by petrography and by Cr_2O_7 oxidation was found in unsealed parking lot dust and residential street dust, which have relatively high contents of asphalt (Figure 3.3). This can be attributed to the overestimation of asphalt-BC in field samples when using BC/OC ratios from reference asphalt materials determined by Cr_2O_7 oxidation. Asphalt in field samples undergoes weathering in sunlight and air. Photooxidation of the lower molecular-weight oil fractions generates more water-soluble asphalt, and makes it more easily attacked by chemical agents (Oliver and Gibson, 1972; Zarkar, 1971); hence, chemical reactions for unweathered reference asphalt material may not be as complete as for weathered asphalt particles in environmental samples.

3.3.6 Contribution of Coal Tar to BC Determined by CTO-375

The CTO-375 results of the reference coal tar and asphalt samples suggest that coal tar likely contributes to BC contents in samples determined with CTO-375, whereas asphalt does not. Hence, we compared the contributions of BC by coal tar and soot in the petrographic results with the total BC determined by CTO-375 in Figure 3.4. The BC contents contributed by coal tar were calculated from the ratio of BC/OC in reference coal tar samples (0.11) (Table B2) and OC in coal tar determined by petrography (Figure 3.1).

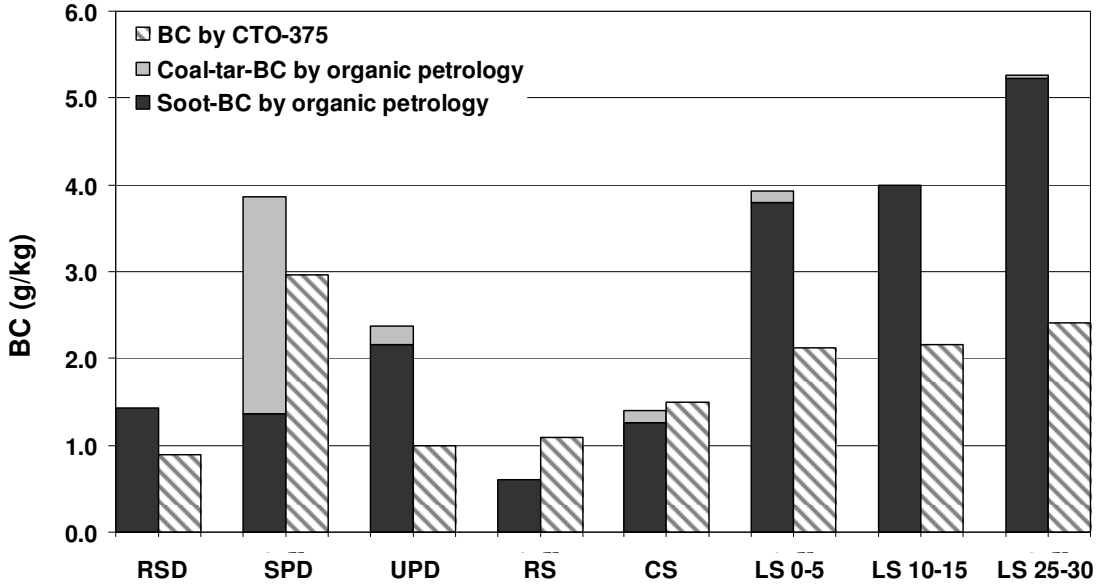

Figure 3.4. The comparison of BC quantified by CTO-375 method to the sum of soot-BC and coal-tar-BC quantified by organic petrography.

The distribution pattern of BC in pavement dust, soils, and sediments estimated by these two methods are similar: BC is higher in sealed parking lot dust and sediments, lower in other samples. The BC content in sealed parking dust estimated by petrography is about 46% of that determined by CTO-375 without considering the contribution of coal tar (Figure 3.2); however, by counting the contribution of coal tar to BC content, the amount of BC in sealed parking lot dust estimated by petrography is closer (within 30%) to that determined by CTO-375 (Figure 3.4). Including coal-tar-BC also results in slightly better agreement between petrographic and CTO-375 measurements of commercial soil-BC. For other samples, agreement is either slightly worse or unaffected.

The sum of soot-BC and coal-tar-BC estimated by petrography is greater than the amount of BC quantified by CTO-375, except for the residential soil and commercial soil

samples. The artifact of CTO-375 that creates BC through inadvertently charring might be responsible for the higher BC contents in two soil samples because relatively more grass debris were observed in these two samples (Nguyen et al., 2004; Masiello, 2004).

The CTO-375 method has been widely applied to quantify the most condensed forms of BC that are highly resistant to thermal treatment (Elmquist et al., 2006; Hammes et al., 2007). Generated during the coking process at 1100 ºC, the thermal recalcitrance of coal tar is expected. Abraham (1961) indicated that certain coal tar carries variable amounts of so-called "free C" when overheated in their process of manufacture, and the "free C" may consist in part of amorphous C, similar to lampblack (oil-soot). Khalil et al. (2006) also reported that a fraction of CTO-375-measured-BC in manufactured gas plant impacted sediments was affected by coal-tar pitch.

3.3.7. Environmental Significance

Asphalt and coal tar are commonly used in infrastructure construction in the urban environment. About 70 billion lb of asphalt is used annually in the U.S. and most often in the construction of roads, parking lots, walkways, and other paved surfaces (Freemantle, 1999). Of the 2.27 million miles of paved road in the United States, 94% are surfaced with asphalt (http://www.encyclopedia.com). Although national use is not reported, the sealcoat industry estimates that in the State of Texas, 225 million L of refined coal-tar-based sealcoat are applied annually; the New York Academy of Sciences reported estimated annual use of coal-tar-based sealcoat in the New York harbor watershed of approximately 5.3 million L (Van Metre et al., 2009). The amount of weathered asphalt and coal tar particles in runoff cannot be neglected, nor can their roles as sources of anthropogenic CMs in urban soils, and sediments of streams, and lakes.

Because of their pyrogeneous origins and chemical and thermal recalcitrance, asphalt and coal tar likely contribute to the pool of BC, although they haven't been considered in the BC continuum. Methods based on chemical and thermal oxidation will possibly overestimate soot-BC and char-BC in urban environmental samples that contain asphalt and coal tar, and result in errors balancing the global BC budget. This overestimation can also lead to a misinterpretation of the role of BC in controlling the transport and fate of organic contaminants in the environment because the affinity of organic contaminants to asphalt and coal tar is different from that to soot. Therefore, caution is advised when measuring BC contents in urban environmental matrices using either chemical or thermal methods. We recommend that for more accurate quantification, organic petrography can be coupled to either chemical or thermal BC quantification methods. However, this approach may fail to count particles smaller than 1.0 μm due to its detection limit (0.2 vol % for particles greater than 1 to 2 μm), and it requires further study using different environmental matrices and calibration against different consensus-BC reference materials.

3.4 References

Brodowski, S., A. Rodionov, L. Haumaier, B. Glaser, W. Amelung, 2005, Revised black carbon assessment using benzene polycarboxylic acids, Organic Geochemistry, 36(9), 1299-1310.

Chambrion, P., R. Bertau, P. Ehrburger, 1995, Effect of polar components on the physico-chemical properties of coal tar, Fuel, 74(9), 1284-1290.

Cornelissen, G., O. Gustafsson, T.D. Bucheli, M.T.O. Jonker, A.A. Koelmans, P.C.M. Van Noort, 2005, Extensive sorption of organic compounds to black carbon, coal, and kerogen in sediments and soils: Mechanisms and consequences for distribution,

bioaccumulation, and biodegradation, Environmental Science and Technology, 39(18), 6881-6895.

Cornelissen, G., Z. Kukulska, S. Kalaitzidis, K. Christanis, O. Gustafsson, 2004, Relations between environmental black carbon sorption and geochemical sorbent characteristics, Environmental Science & Technology, 38(13), 3632-3640.

Dickens, A.F., Y. Gelinas, C.A. Masiello, S. Wakeham, J.I. Hedges, 2004, Reburial of fossil organic carbon in marine sediments, Nature, 427(6972), 336-339.

Durand, B., G. Nicaise, 1980, Procedures for Kerogen Isolation, Paris, Editions Technip.,

Elmquist, M., G. Cornelissen, Z. Kukulska, O. Gustafsson, 2006, Distinct oxidative stabilities of char versus soot black carbon: Implications for quantification and environmental recalcitrance, Global Biogeochemical Cycles, 20(2), GB2009.

Elmquist, M., O. Gustafsson, P. Andersson, 2004, Quantification of sedimentary black carbon using the chemothermal oxidation method: an evaluation of ex situ pretreatments and standard additions approaches, Limnology And Oceanography-Methods, 2, 417-427.

Forbes, M.S., R.J. Raison, J.O. Skjemstad, 2006, Formation, transformation and transport of black carbon (charcoal) in terrestrial and aquatic ecosystems, Science of The Total Environment, 370(1), 190-206.

Freemantle, M., 1999, What's that Stuff? -Asphalt: A sticky subject, Chemial & Engineering News, 77(47), 81-82.

Gelinas, Y., K.M. Prentice, J.A. Baldock, J.I. Hedges, 2001, An improved thermal oxidation method for the quantification of soot/graphitic black carbon in sediments and soils, Environmental Science & Technology, 35(17), 3519-3525.

Goldberg, E.D., 1985, Black Carbon in the Environment: Properties and Distribution, John Wiley & Sons: New York, A Wiley-Interscience Publication.

Gustafsson, O., T.D. Bucheli, Z. Kukulska, M. Andersson, C. Largeau, J.N. Rouzaud, C.M. Reddy, T.I. Eglinton, 2001, Evaluation of a protocol for the quantification of black carbon in sediments, Global Biogeochemical Cycles, 15(4), 881-890.

Gustafsson, O., P.M. Gschwend, 1997, Soot as a strong partition medium for polycyclic aromatic hydrocarbons in aquatic systems, Molecular Markers In Environmental Geochemistry, 671,365-381.

Gustafsson, O., P.M. Gschwend, 1998, The flux of black carbon to surface sediments on the New England continental shelf, Geochimica et Cosmochimica Acta, 62(3), 465-472.

Gustafsson, O., F. Haghseta, C. Chan, J. MacFarlane, P.M. Gschwend, 1997, Quantification of the dilute sedimentary soot phase: Implications for PAH speciation and bioavailability, Environmental Science & Technology, 31(1), 203-209.

Hammes, K., M.W.I. Schmidt, R.J. Smernik, L.A. Currie, W.P. Ball, T.H. Nguyen, P. Louchouarn, S. Houel, O. Gustafsson, M. Elmquist, G. Cornelissen, J.O. Skjemstad, C.A. Masiello, J. Song, P. Peng, S. Mitra, J.C. Dunn, P.G. Hatcher, W.C. Hockaday, D.M. Smith, C. Hartkopf-Froeder, A. Boehmer, B. Luer, B.J. Huebert, W. Amelung, S. Brodowski, L. Huang, W. Zhang, P.M. Gschwend, D.X. Flores-Cervantes, C. Largeau, J.N. Rouzaud, C. Rumpel, G. Guggenberger, K. Kaiser, A. Rodionov, F.J. Gonzalez-Vila, J.A. Gonzalez-Perez, J.M. de la Rosa, D.A. C. Manning, E. Lopez-Capel, L. Ding, 2007, Comparison of quantification methods to measure fire-derived (black/elemental) carbon in soils and sediments using reference materials from soil, water, sediment and the atmosphere, Global Biogeochemical Cycles, 21(3), GB3016.

Hedges, J.I., G. Eglinton, P.G. Hatcher, D.L. Kirchman, C. Arnosti, S. Derenne, R.P. Evershed, I. Kogel-Knabner, J.W. de Leeuw, R. Littke, W. Michaelis, J. Rullkotter, 2000, The molecularly-uncharacterized component of nonliving organic matter in natural environments, Organic Geochemistry, 31(10), 945-958.

Jeong, S., M.M. Wander, S. Kleineidam, P. Grathwohl, B. Ligouis, C.J. Werth, 2008, The role of condensed carbonaceous materials on the sorption of hydrophobic organic contaminants in subsurface sediments, Environmental Science & Technology, 42(5), 1458-1464.

Jeong, S., C.J. Werth, 2005, Evaluation of methods to obtain geosorbent fractions enriched in carbonaceous materials that affect hydrophobic organic chemical sorption, Environmental Science & Technology, 39(9), 3279-3288.

Jonker, M.T.O, A.A. Koelmans, 2002, Sorption of polycyclic aromatic hydrocarbons and polychlorinated biphenyls to soot and soot-like materials in the aqueous environment mechanistic considerations, Environmental Science & Technology, 36(17), 3725-3734.

Jonker, M.T.O, F. Smedes, 2000, Preferential Sorption of Planar Contaminants in Sediments from Lake Ketelmeer, The Netherlands, Environ. Sci. Technol., 34(9), 1620-1626.

Khalil, M.F., U. Ghosh, J.P. Kreitinger, 2006, Role of weathered coal tar pitch in the partitioning of polycyclic aromatic hydrocarbons in manufactured gas plant site sediments, Environmental Science & Technology, 40(18), 5681-5687.

Kuhlbusch, T.A.J., 1998, Black carbon and the carbon cycle, Science, 280(5371), 1903-1904.

Kuo, L.J., B.E. Herbert, P. Louchouarn, 2008, Can levoglucosan be used to characterize and quantify char/charcoal black carbon in environmental media?, Organic Geochemistry, 39(10), 1466-1478.

Liang, B., J. Lehmann, D. Solomon, S. Sohi, J.E. Thies, J.O. Skjemstad, F.J. Luizão, M.H. Engelhard, E.G. Neves, S. Wirick, 2008, Stability of biomass-derived black carbon in soils, Geochimica et Cosmochimica Acta, 72(24), 6069-6078.

Lim, B., H. Cachier, 1996, Determination of black carbon by chemical oxidation and thermal treatment in recent marine and lake sediments and Cretaceous-Tertiary clays, Chemical Geology, 131(1-4), 143-154.

Mahler, B.J., P.C. Van Metre, T.J. Bashara, J.T. Wilson, D.A. Johns, 2005, Parking lot sealcoat: An unrecognized source of urban polycyclic aromatic hydrocarbons, Environmental Science & Technology, 39(15), 5560-5566.

Masiello, C.A., 2004, New directions in black carbon organic geochemistry, Marine Chemistry, 92(1-4), 201-213.

Masiello, C.A, E.R.M. Druffel, 1998, Black carbon in deep-sea sediments, Science, 280(5371), 1911-1913.

Masiello, C.A., E.R.M. Druffel, L.A. Currie, 2002, Radiocarbon measurements of black carbon in aerosols and ocean sediments, Geochimica Et Cosmochimica Acta, 66(6), 1025-1036.

Nguyen, T.H., R.A. Brown, W.P. Ball, 2004, An evaluation of thermal resistance as a measure of black carbon content in diesel soot, wood char, and sediment, Organic Geochemistry, 35(3), 217-234.

Oliver, J.W., H.H. Gibson, 1972, Source of Water-soluble Photooxidation Products in Asphalt, Industrial & Engineering Chemistry Product Research and Development, 11(1), 66-69.

Peters, C.A., R.G. Luthy, 1993, Coal-Tar Dissolution In Water-Miscible Solvents - Experimental Evaluation, Environmental Science & Technology, 27(13), 2831-2843.

Schmidt, M.W., I.A.G. Noack, 2000, Black carbon in soils and sediments: Analysis, distribution, implications, and current challenges, Global Biogeochemical Cycles, 14(3), 777-793.

Schmidt, M.W.I., J.O. Skjemstad, C.I. Czimczik, B. Glaser, K.M. Prentice, Y. Gelinas, T.A.J. Kuhlbusch, 2001, Comparative analysis of black carbon in soils, Global Biogeochemical Cycles, 15(1), 163-167.

Song, J.Z., P.A. Peng, W.L. Huang, 2002, Black carbon and kerogen in soils and sediments. 1. Quantification and characterization, Environmental Science & Technology, 36(18), 3960-3967.

Swift, R.S., D.L. Sparks, 1996, Organic Matter Characterization, Madison, Soil Sci. Soc. Am.

Taylor, G.H., M. Teichmuller, A. Davis, C.F.K. Diessel, R. Littke, P. Robert, 1998, *Organic Petrology*, Berlin, Gebrüder Borntraeger.

Van Metre, P.C., B.J. Mahler, J.T. Wilson, 2009, PAHs underfoot: Contaminated dust from coal-tar sealcoated pavement is widespread in the United States, Environmental Science & Technology, 43(1), 20-25.

Zakar, P., 1971, Asphalt, New York, Chemical Publishing Company, Inc.

SIC 2951 Asphalt Paving Mixtures and Blocks, 2005, Encyclopedia of American Industries, The Gale Group, Inc., http://www.encyclopedia.com, accessed on April 16, 2009.

Chapter 4

Phenanthrene Sorption by Carbonaceous Materials in Urban Dust, Soils, and Sediments Containing Asphalt and Coal Tar

4.1 Introduction

Sorption to carbonaceous materials (CMs) is an important process controlling the transport and fate of hydrophobic organic compounds (HOCs) in the environment. Over the last several decades, extensive research has been done to expand our understanding of sorption interactions between HOCs and CMs. Sorption not only depends on the amount of CMs present in a soil or sediment, but also the nature of CMs (Grathwohl, 1990; Jonker and Koelmans, 2001; Karapanagioti et al., 2000; Kleineidam et al., 1999; Kleineidam et al., 2002).

Numerous investigators have shown that various CMs have distinct sorption properties and capacities due to their different origin and geological history. Sorption to more condensed form of CMs like kerogen (Grathwohl, 1990) and soot (Ghosh et al., 2000) is more favorable than sorption to more labile recent OM. Kleineidam et al. (1999) found that kerogen in sedimentary rock sorbs more phenanthrene than relatively recent organic matter (OM) in soils, and Jonker and Koelmans (2001, 2002) found that soot sorbs 10-1000 times more polycyclic aromatic hydrocarbons (PAHs) per unit weight of sorbent than amorphous sedimentary OM. One form of a "dual-mode" model was developed and modified to describe the sorption of HOCs to sediments and soils (Accardi-Dey and Gschwend, 2002; Gustafsson et al., 1997; Xia and Ball, 1999). According to this model, CMs in the soils and sediments consist of two domains: 1) soft amorphous CMs showing linear and noncompetitive absorption (Huang et al., 1997;

Pignatello and Xing, 1996), and 2) hard condensed CMs that show nonlinear, extensive and competitive adsorption (Huang et al., 1997; Xia and Ball, 1999). The total HOC sorption can then be expressed as a superposition of partitioning and adsorption. Sequestration and slow desorption of HOCs are presumed to be dominated by retention within condensed CMs (CCMs) (Abu and Smith, 2005).

Humin, kerogen, and black carbon (BC) (including char/charcoal and soot) are usually considered as CCMs according to their origins and experiment-based definitions (Pan et al., 2006; Ran et al., 2007a, 2007b). Our results in Chapter 2 showed that asphalt and coal tar are ubiquitous in urban dust, soils, and sediments, and pyrogenic asphalt and coal tar are resistant to Cr_2O_7 oxidation and may contribute to BC measurements in samples from urban areas (Chapter 3); therefore, asphalt and coal tar may contribute to the sorption capacities of the CCMs and influence their sorption properties. Recently, the influence of coal-tar pitch on PAH sorption in sediments has been studied (Bayard et al., 2000; Benhabib et al., 2006; Breedveld et al., 2007; Khalil et al., 2006). Khalil et al. (2006) developed a pitch-partitioning inclusive model to describe PAH partitioning behavior in sediments that contain significant quantities of pitch residue, and indicated that the partitioning behavior may be dominated by the sorption characteristics of pitch and not by natural OM or BC.

The objective of this study is to investigate the correlation between CM properties and their corresponding sorption affinity to PAHs, and to evaluate the influence of asphalt and coal tar on PAH sorption to CMs in urban dust, soils, and sediments. A better understanding of how CM properties influence sorption abilities will make it possible to predict PAH sorption to CM particles in complex environmental matrices, to determine

the primary mechanisms that control the redistribution and persistence of PAHs in urban watersheds, and to assess the associated environmental risks of contaminated sediments.

4.2 Materials and Methods

4.2.1 Sample Collection

Samples were collected from Lake Como watershed, Fort Worth, Texas, including one street dust sample, two parking lot dust samples, two surface soil samples, and three lake sediment samples. The street dust sample was a composite of dust from three asphalt-paved residential streets. One parking lot dust sample was a composite of dust from three coal-tar-sealed commercial parking lots and the other was a composite of dust from three unsealed asphalt or cement commercial parking lots. Two surface soil samples (top 2 cm) were collected randomly at approximately 40 locations near roads, sidewalks and driveways; one was from a residential neighborhood and the other was from a commercial area. Three sediment cores several meters apart were collected from a single site in Lake Como using a box corer. The cores were vertically extended and sliced at 5-cm intervals, and subsamples from the same depths (depth from the top: 0-5 cm, 10-15 cm, and 25-30 cm) were combined from the three cores to create three large-volume samples. Each composite sample was homogenized after passing through a 1-mm sieve. Details of the Lake Como sampling site and sample collection methods were described in Chapter 2.

4.2.2 Density Separation

Representative sub-samples of Lake Como watershed field samples were separated into light (LFr) and heavy (HFr) fractions with a solution of 1.60 g/cm^3 sodium polytungstate. Both fractions were oven dried at 60ºC, pulverized, and passed through a 100-mesh sieve to enhance reaction kinetics of subsequent chemical and thermal treatments.

4.2.3 CCM Separation

The fractions enriched in CCMs were obtained by treating HFr fractions sequentially with HCl, HF/HCl, trifluoroacetic acid (TFA)/HCl, and sodium hydroxide (NaOH) to remove carbonates, silicate minerals (Durand, 1980), easily hydrolyzable OM (Gelinas et al., 2001), and fulvic and humic acids (Swift, 1996), respectively. The remaining residues were referred to as HFr-CCM fractions in this report. Procedures were the same as described in Jeong et al. (Jeong et al., 2008; Jeong and Werth, 2005).

4.2.4 Sample Characterization

The specific surface area (SSA) of bulk samples and HFr and LFr fractions were measured with the multipoint Brunauer-Emmet-Teller (BET) method using an Accelerated Surface Area and Porosimetry system (ASAP 2010).

The C and hydrogen (H) contents of bulk samples, HFr and LFr fractions, and the HFr-CCM fractions were determined using a CE 440 CHN analyzer (Exeter Analytical, Inc., North Chelmsford, MA) in the Microanalysis Laboratory at the University of Illinois at Urbana-Champaign (UIUC), after the removal of inorganic C followed by oven drying. The oxygen (O) analysis was measured using a Leco RO-478 oxygen analyzer (Leco

Corp., St. Joseph, MI) at Huffman Laboratories, Inc. (Golden, CO) following ASTM D5622.

Surface functional groups were analyzed with a diffuse reflectance Fourier transform infrared (DR-FTIR) spectrometer (Nexus 670 FT-IR, Thermo Nicolet Co.) equipped with a deuterated triglycine sulfate (DTGS) detector following Wander and Traina (1996). Powdered bulk samples and HFr-CCM fractions were mixed with powdered KBr until homogeneous and then analyzed with a constant flow of dried air in order to minimize infrared absorption by water vapor. DR-FTIR spectra were obtained using 500 scans collected at 4 cm^{-1} resolution from 4000 to 400 cm^{-1} and analyzed with OMNIC software (Thermo Nicolet Co., Fitchburg, WI).

4.2.5 Sorption Experiment

Sorption isotherms were measured using established batch equilibrium methods (e.g. Chiou and Kile, 1998; Xia and Ball, 1999; Xing et al., 1996) with ^{14}C- phenanthrene (Sigma-Aldrich, St. Louis, MO) as the sorbate to distinguish spiked sorbate from background contaminants. Sorbents include bulk samples, LFr and HFr fractions, and HFr-CCM fractions. ^{14}C-phenanthrene was used as received, and the purities and specific activities are 99+% and 8.2 mCi/mmol. Sorption experiments were conducted in 30-mL glass centrifuge tubes with PTFE-lined solid phenolic screw caps. The mass of a sorbent added to each tube was adjusted to achieve 20-70% uptake of sorbate. After the sorbent was saturated with background solution containing 0.005 M $CaCl_2$ and 0.02% NaN_3 (by weight) overnight, a stock solution of sorbate in methanol (1-25 μL) was injected into the tubes. The spiked solutions were always at or below 0.1% of the total volume in the tubes to minimize cosolvent effects (Gossett, 1987). Tubes were capped immediately after

stock solution injection and then tumbled end-over-end at 1 rpm in a dark room at 25°C. Preliminary experiments were performed to determine the period of time needed to achieve apparent sorption equilibrium. After establishment of sorption equilibrium, sorbents and aqueous phases were separated by centrifugation at 6500 rpm (rcf =6116 g) for 30 min, and 2.5 mL of supernatant was taken for scintillation counting (LS3801, Beckman Instruments, Fullerton, CA) to determine the remaining ^{14}C- phenanthrene in aqueous phase. The amount of sorbate in the sorbed phase was calculated by the difference between the amount initially added and that remaining in the solution.

The sorption data were fit with both the Freudnlich isotherm model (Eq 1) and the linear partitioning model (Eq 2):

$$logC_S = logK_F + N\ logC_W \qquad \text{(Eq 1)}$$

$$C_S = K_D C_W \qquad \text{(Eq 2)}$$

where C_S is the solid-phase concentration (μg/kg) and C_W is the aqueous concentration (μg/L); K_F is the Freundlich solid-water distribution coefficient [(μg/kg)/(μg/L)^N]; K_D is the linear solid-water partition coefficient (L/kg); and N is the Freundlich exponent.

The sorption contributions of CM fractions to bulk samples were determined by assuming that, at a fixed aqueous concentration, the mass sorbed to each fraction i is the same when this fraction is alone, or part of the bulk sample. Mathematically, we define the sorption contribution of fraction i at a given concentration C as:

$$Sorption\ \ Contribution\ \ of\ \ Fraction\ \ i = \frac{C_{S,i}}{C_{S,bulk}} \times 100\% \qquad \text{(Eq 3)}$$

where $C_{S,i} = K_{F_i} C^{N_i} \times m_i$

and m_i is the mass percentage of fraction i in bulk samples.

4.3 Results and Discussions

4.3.1 Properties of CMs

As illustrated in Chapter 3, the OC contents in LFr fractions are higher than in HFr fractions (Table 4.1), but the majority of OC is associated with HFr (52 – 98%) due to the dominant mass in HFr fractions (Figure 4.1). The OC contents in HFr-CCM fractions range from 51.2% to 72.5% and account for 25 – 68% of the OC in bulk samples, with the highest value in sealed parking lot dust. The H/C atomic ratios range from 0.44 to 0.76 in bulk samples, 0.13 to 0.83 in HFr fractions, 0.10 to 0.17 in LFr fractions, and 0.07 to 0.11 in HFr-CCM fractions. The O/C ratios of HFr-CCM fractions range from 0.10 to 0.47, lower than the average O/C ratios (0.53) for typical humic substances extracted from soils and sediments (Wang and Xing, 2005), suggesting a higher degree of maturation than humic substances; however, the O/C ratios of HFr-CCM fractions are higher than those of BC in soil samples determined with combustion at 375ºC by Ran et al. (2007b) (0.078-0.13), indicating that the degree of maturation of HFr-CCM fractions is lower than BC.

Table 4.1. Physicochemical properties of bulk samples, LFr and HFr fractions, and HFr-CCM fractions (LS 0-5, LS 10-15, LS 25-30, RS, CS, RSD, SPD, and UPD represent lake sediments from 0-5 cm depth, lake sediments from 10-15 cm depth, lake sediments from 25-30 cm depth, residential soil, commercial soil, residential street dust, sealed parking lot dust, and unsealed parking lot dust, respectively).

Sample ID	Fraction	OC (%)	H (%)	O (%)	H/C	O/C	SSA (m^2/g)
RSD	Bulk	2.87	1.39	nd*	0.49	nd	0.67
	LFr	38.58	5.73	nd	0.15	nd	0.59
	HFr	1.53	1.26	nd	0.83	nd	1.20
	HFr-CCM	63.22	6.81	10.68	0.11	0.17	nd
SPD	Bulk	4.20	2.33	nd	0.55	nd	0.20
	LFr	39.71	4.09	nd	0.10	nd	0.35
	HFr	3.64	0.47	nd	0.13	nd	0.75
	HFr-CCM	72.45	4.81	7.54	0.07	0.10	nd
UPD	Bulk	2.78	1.31	nd	0.47	nd	0.49
	LFr	34.30	5.15	nd	0.15	nd	0.51
	HFr	1.55	0.97	nd	0.63	nd	1.02
	HFr-CCM	65.64	6.85	9.73	0.10	0.15	nd
RS	Bulk	2.80	1.22	nd	0.44	nd	3.09
	LFr	26.14	4.27	nd	0.16	nd	1.23
	HFr	2.10	0.31	nd	0.15	nd	2.77
	HFr-CCM	54.46	5.73	17.93	0.11	0.33	nd
CS	Bulk	4.00	2.44	nd	0.61	nd	5.24
	LFr	31.14	4.26	nd	0.14	nd	1.37
	HFr	3.20	0.63	nd	0.20	nd	3.41
	HFr-CCM	51.22	4.73	24.19	0.09	0.47	nd
LS 0-5	Bulk	3.92	2.33	nd	0.59	nd	9.17
	LFr	26.20	4.37	nd	0.17	nd	2.33
	HFr	3.55	2.14	nd	0.60	nd	7.16
	HFr-	59.67	6.17	16.82	0.10	0.28	nd
LS 10-15	Bulk	4.71	2.35	nd	0.50	nd	9.31
	LFr	23.90	3.71	nd	0.16	nd	2.78
	HFr	4.13	2.02	nd	0.49	nd	6.81
	HFr-CCM	62.88	6.68	16.85	0.11	0.27	nd
LS 25-30	Bulk	5.04	3.83	nd	0.76	nd	7.76
	LFr	27.00	4.19	nd	0.16	nd	2.80
	HFr	4.99	2.44	nd	0.49	nd	6.68
	HFr-CCM	62.91	6.76	16.02	0.11	0.25	nd

* nd: not determined.

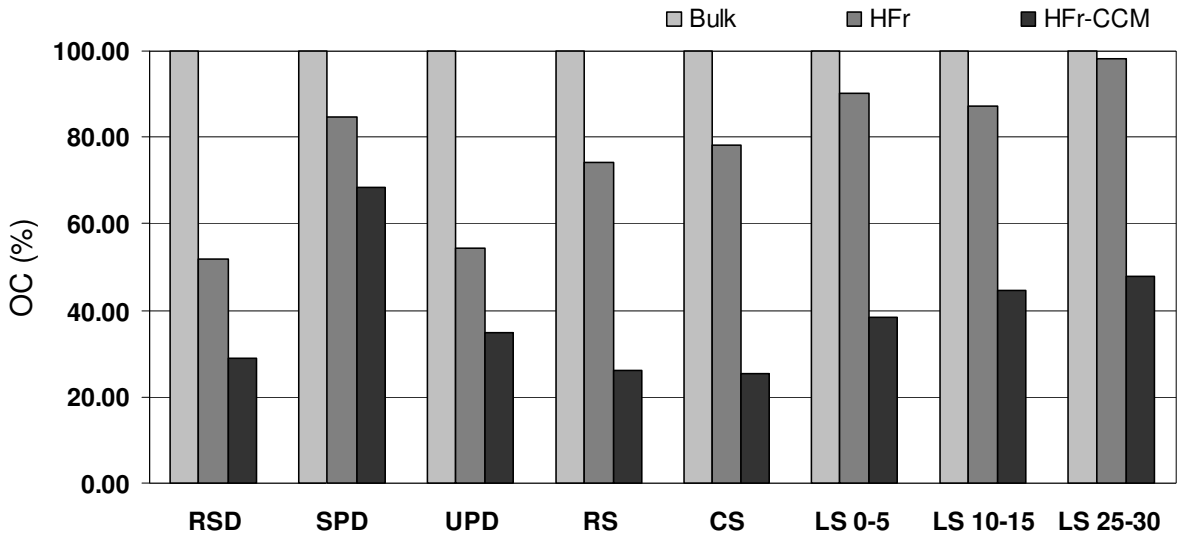

Figure 4.1. The percentages of OC contributed by HFr-CCM and HFr fractions to bulk samples from Lake Como watershed.

SSA of bulk samples, LFr and HFr fractions, and HFr-CCM fractions all follow the same trend: lake sediment > soil > dust, but no trend was observed for different fractions of the same sample (Table 4.1). The greatest SSA in bulk sediment samples is likely due to the presence of relatively large amounts of clay minerals. Bulk dust samples (e.g., residential street, sealed parking lot, and unsealed parking lot dust) have the lowest SSA. This makes sense because asphalt and coal tar pitch have low porosity, and petrographic analysis results (Chapter 2) show that these materials are the dominant CMs in dust samples from residential streets and sealed and unsealed parking lots.

DR-FTIR spectra of bulk samples and HFr-CCMs are shown in Figures 4.2 and 4.3. The spectra of all bulk samples are quite similar in terms of peak positions and relative intensities. All bulk samples have peaks derived from alcohol and phenol O-H stretching (3640-3610 cm-1), methyl C-H stretching (2920 cm-1), methylene C-H

stretching (2850 cm-1), carboxylic acid O-H stretching (~2500 cm-1), C=O stretching (~1800 cm-1), conjugated aromatic systems (1590~1610 cm-1), aliphatic C-H bending (~1450 cm-1), C-O stretching (1040-1300 cm-1), and aromatic out of plane bending with different degrees of substitution (900-700 cm-1) (Jeong and Werth, 2005; Ran et al., 2007b) (Figure 4.2).

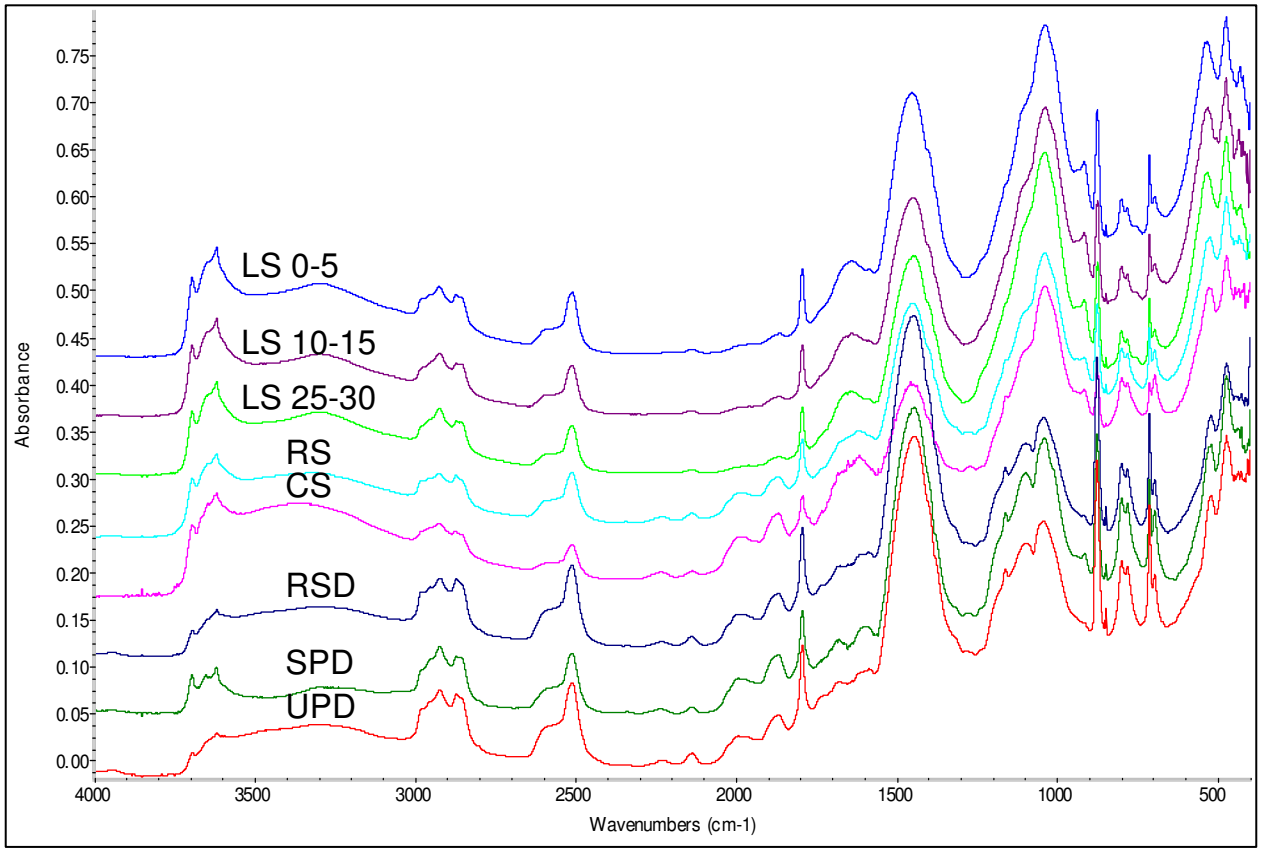

Figure 4.2. DR-FTIR spectra of bulk samples from Lake Como watershed.

DR-FTIR spectra of HFr-CCM fractions (Figure 4.3) are markedly different from those of the bulk samples (Figure 4.2). The spectra of HFr-CCM fractions for soils and sediments are generally similar, and those for the three dust samples are similar. For

sealed parking lot samples, a significant difference can be observed regarding the location of aromatic C-H stretching peak (3100-3000 cm-1), indicating the abundance of aromatic compounds in coal-tar pitch. Consistent with Ran et al. (2007b), after chemical treatment with HF/HCl, TFA, and NaOH, peaks for the aliphatic (2920 and 2850 cm-1) and conjugated aromatic groups (1590~1610 cm-1) are stronger than other groups. The aromatic carbonyl/carboxyl C=O stretching (1704 cm-1) indicates the condensed CMs have some aromatic acids and aldehydes. Although this peak is weaker than nearby conjugated aromatic systems (1590~1610 cm-1) in soil and sediment samples, the difference is smaller in dust samples, suggesting that dust samples have relatively more aromatic acids and aldehydes. The aromatic out of plane bending (900-700 cm-1) is obviously stronger in dust samples, similar to the signature peaks observed in coal tar pitch and asphalt in a previous study (Alcaniz-Monge et al., 2001). However, the relative intensities of these peaks among three dust samples are not the same. The peak at 800 cm-1 is more intense in the sealed parking lot dust than in residential street dust and unsealed parking lot dust. This may indicate the difference of the relative abundance of coal tar and asphalt in these samples.

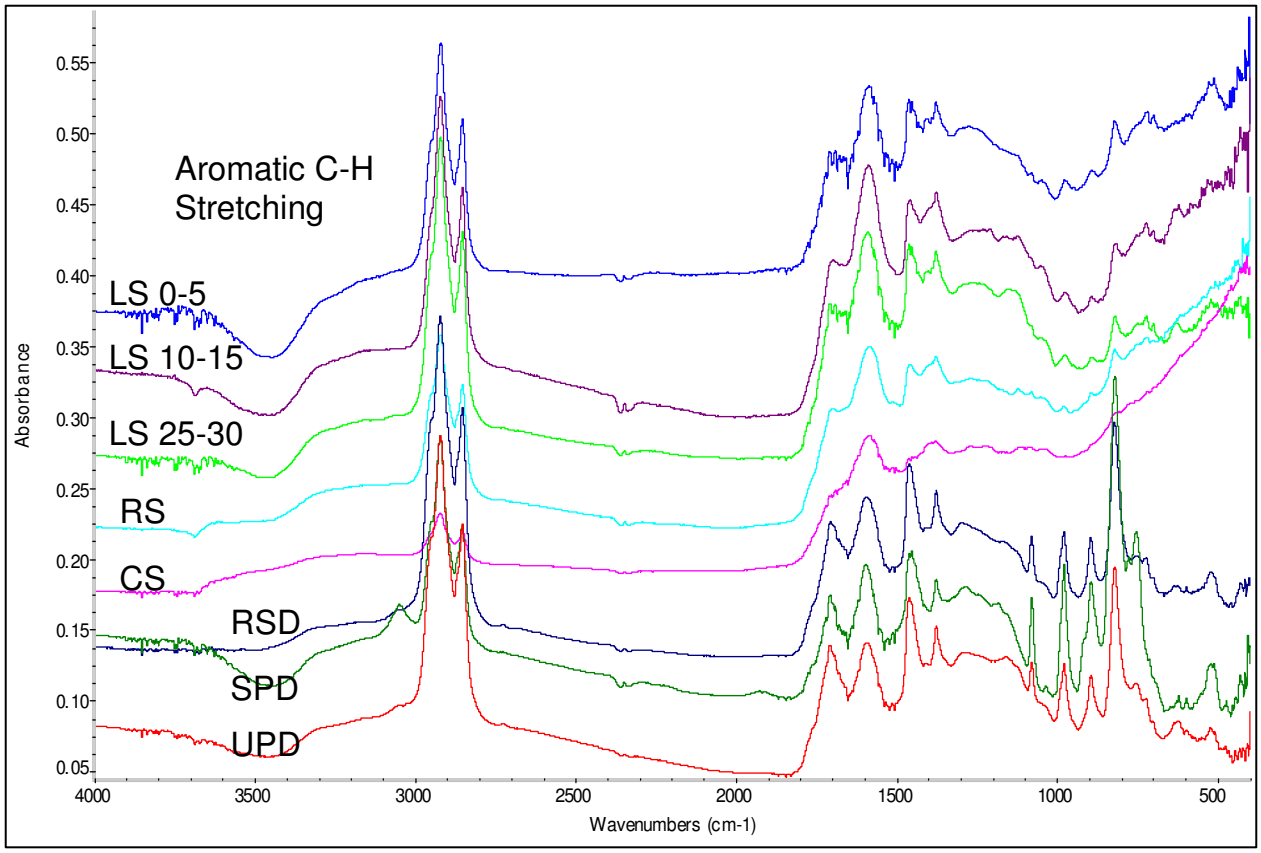

Figure 4.3. DR-FTIR spectra of HFr-CCM fractions for samples from Lake Como watershed (LS 0-5, LS 10-15, LS 25-30, RS, CS, RSD, SPD, and UPD represent lake sediment at depth of 0-5 cm, lake sediment at depth of 10-15 cm, lake sediment at depth of 25-30 cm, residential soil, commercial soil, residential street dust, sealed parking lot dust, and unsealed parking lot dust, respectively).

4.3.2 Sorption Isotherms

Freundlich and linear isotherm parameters and OC normalized sorption coefficients of bulk samples, LFr and HFr fractions, and HFr-CCM fractions from the Lake Como watershed are presented in Table 4.2. All sorption isotherms are nearly linear with N values between 0.90 and 1.00. This indicates partitioning is the dominant sorption mechanism. Freundlich constants (K_F) of LFr fractions are greater than those of HFr fractions and bulk samples due to the high OC contents in LFr fractions. The Freundlich sorption coefficients (K_F) of HFr-CCMs are about 16-45 times of those of HFr fractions,

Table 4.2. Sorption isotherm parameters of bulk samples, LFr and HFr fractions, and HFr-CCM fractions of Lake Como watershed samples.

Sample ID		$logK_F$ $(\mu g/kg)/(\mu g/L)^N$	N	R_F^2	$logK_D$ (L/kg)	R_D^2	$log\ Koc$ $(L/kg\ C)$
RSD	Bulk	3.13	0.93	0.995	2.99	0.995	4.54
	LFr	3.89	0.99	0.985	4.03	0.984	4.45
	HFr	3.11	0.93	0.996	2.94	0.999	4.76
	HFr-CCM	4.79	0.99	0.992	4.70	0.990	4.90
SPD	Bulk	3.57	0.94	0.995	3.48	0.999	4.86
	LFr	4.20	0.94	0.989	4.10	0.999	4.50
	HFr	3.47	0.94	0.992	3.40	0.992	4.83
	HFr-CCM	4.67	1.00	0.998	4.70	0.999	4.84
UPD	Bulk	2.97	1.00	0.996	2.96	0.999	4.51
	LFr	4.06	0.95	0.983	4.06	0.995	4.53
	HFr	3.05	0.97	0.994	3.00	0.999	4.81
	HFr-CCM	4.76	0.99	0.996	4.80	0.995	4.99
RS	Bulk	2.79	0.95	0.980	2.70	0.999	4.25
	LFr	3.86	0.93	0.990	3.65	0.995	4.23
	HFr	2.91	0.90	0.977	2.75	0.999	4.43
	HFr-CCM	4.70	0.96	0.997	4.61	0.998	4.87
CS	Bulk	2.96	0.94	0.969	3.04	0.993	4.44
	LFr	3.83	0.96	0.981	3.92	0.992	4.42
	HFr	3.00	0.93	0.972	3.02	0.994	4.52
	HFr-CCM	4.56	0.98	0.997	4.54	0.999	4.83
LS 0-5	Bulk	3.30	0.91	0.998	3.03	0.997	4.43
	LFr	4.26	0.91	0.996	4.08	0.977	4.66
	HFr	3.24	0.93	0.999	3.03	0.996	4.48
	HFr-CCM	4.88	0.94	0.997	4.68	0.994	4.90
LS 10-15	Bulk	3.38	0.97	0.999	3.31	0.989	4.63
	LFr	4.28	0.91	0.995	4.12	0.999	4.74
	HFr	3.34	0.95	0.999	3.17	0.997	4.55
	HFr-CCM	4.79	0.99	0.998	4.73	0.995	4.93
LS 25-30	Bulk	3.43	0.96	0.998	3.35	0.997	4.65
	LFr	4.23	0.92	0.996	3.99	0.975	4.56
	HFr	3.36	0.98	0.997	3.32	0.999	4.62
	HFr-CCM	4.76	1.00	0.996	4.67	0.996	4.88

and up to 81 times greater than those of bulk samples, largely due to the enriched OC contents of these samples. The K_{oc} values of HFr-CCM are about 1.4-2.8 times greater than those of HFr fractions, and approximately equal to those for the sealed parking lot dust sample. This implies that the CCMs occupy a larger fraction of the HFr in sealed parking lot dust than in other samples, consistent with results in Figure 4.1, which shows the highest OC mass in sealed parking lot dust after treatment through NaOH extraction. For soil and dust samples, OC normalized sorption coefficients (K_{oc}) are higher in HFr fractions than in LFr fractions, indicating more geologically mature CMs may be associated with HFr fractions (Kleineidam et al., 1999). The greater K_{oc} values for the bulk and HFr fraction of the sealed parking lot dust could also account for the higher PAH concentrations in this sample, in addition to the original contributions from the coal-tar pitch sealcoat (Chapter 2).

4.3.3 Contribution of CM Fractions to Phenanthrene Sorption

The sorption contributions of HFr-CCM and HFr fractions to bulk samples at the equilibrium concentration of 10 μg/L are shown in Figure 4.4. The equilibrium concentration of 10 μg/L was chosen based on the PAH source study by Mahler et al. (2005). They reported that the concentrations of dissolved PAHs in runoff from coal tar sealed parking lots ranged from 2.3-16 μg/L. The sorption contributions of untreated HFr fractions to the bulk samples are greater than 77% due to their relatively large mass contents and OC contents. Sorption contributions over 100% suggest that CMs with higher sorptivity may have been exposed by physical shaking during density separation. The sorption contributions of the HFr-CCM frations to the bulk samples are between

57% and 97%, and six of eight samples are above 80%. Hence, sorption of phenanthrene to the bulk samples is controlled by sorption to the CCMs in the HFr fractions.

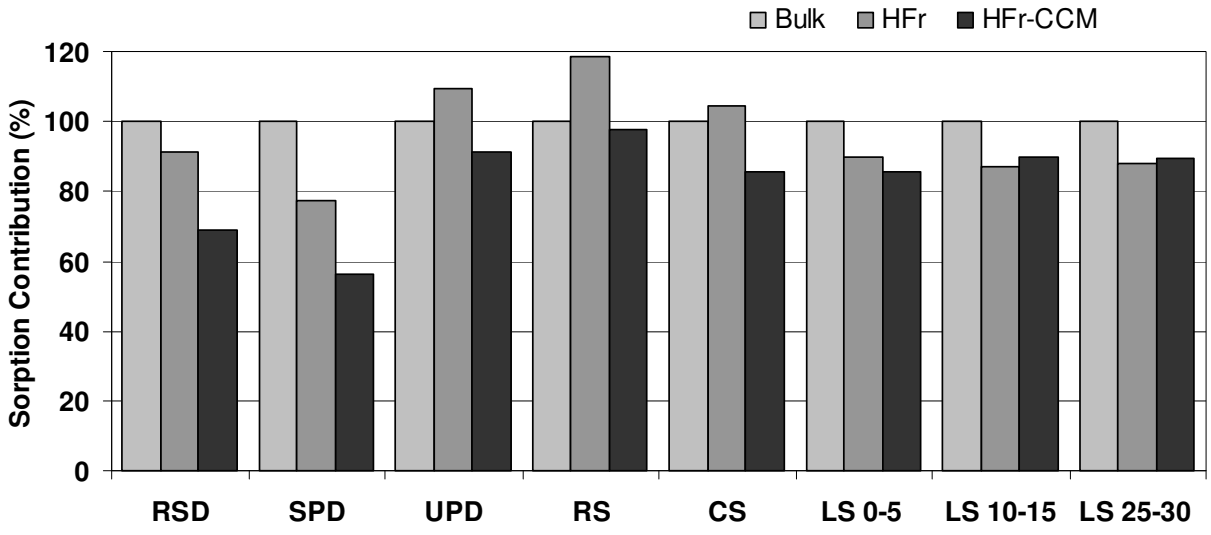

Figure 4.4. Sorption contribution by HFr and HFr-CCM fractions to Lake Como watershed samples at an equilibrium concentration of Ce = 10 ug/L.

4.3.4 Influence of Asphalt and Coal Tar on Sorption

Parameters of CM properties such as H/C and O/C values of bulk samples, LFr and HFr fractions, and HFr-CCM fractions were compared to the sorption coefficients ($logK_F$ and $logK_{OC}$) and no statistically relevant correlations were observed (not shown). This implies that sorption properties of our samples are not controlled by the degree of CM maturation, which is estimated with H/C and O/C ratios (Ran et al., 2007b).

SSA values of bulk samples, LFr, and HFr fractions, and HFr-CCM fractions were also compared to the sorption coefficients and no statistically relevant correlations were observed either (not shown). This suggests that surface adsorption is not the

dominant sorption mechanism in our samples, consistent with the linear sorption isotherms of all samples and fractions. The partitioning-dominated sorption mechanism likely is attributed to the contribution of asphalt and coal tar to overall sorption. The asphalt-water and coal-tar-water distribution coefficients for phenanthrene are $10^{5.7}$ and $10^{5.3}$ L/kg, respectively (Brandt and De Groot, 2001; Endo and Schmidt, 2006), about one order of magnitude higher than amorphous OM-water distribution coefficient ($10^{4.3}$ L/kg) (Schwarzenbach et al., 2003), but 2 and 5 times lower than soot-water distribution coefficients, e.g., a value of $10^{5.93}$ L/kg was measured for traffic soot (Jonker and Koelmans, 2002). The overall sorption of phenanthrene can be dominated by partitioning to amorphous OM, asphalt, and coal tar due to their high contents in our samples.

4.4 References

Abu, A., S. Smith, 2005, Assessing sequestration of selected polycyclic aromatic hydrocarbons by use of adsorption modeling and temperature-programmed desorption, Environmental Science and Technology, 39(19), 7585-7591.

Accardi-Dey, A.P. M. Gschwend, 2002, Assessing the combined roles of natural organic matter and black carbon as sorbents in sediments, Environmental Science and Technology, 36(1), 21-29.

Alcaniz-Monge, J., D. Cazorla-Amoros, A. Linares-Solano, 2001, Characterisation of coal tar pitches by thermal analysis, infrared spectroscopy and solvent fractionation, Fuel, 80(1), 41-48.

Bayard, R., L. Barna, B. Mahjoub, R. Gourdon, 2000, Influence of the presence of PAHs and coal tar on naphthalene sorption in soils, Journal Of Contaminant Hydrology, 46(1-2), 61-80.

Benhabib, K., M.O. Simonnot, M. Sardin, 2006, PAHs and organic matter partitioning and mass transfer from coal tar particles to water, Environmental Science & Technology, 40(19), 6038-6043.

Brandt, H.C., A.P.C. De Groot, 2001, Aqueous leaching of polycyclic aromatic hydrocarbons from bitumen and asphalt, Water Research, 35(17), 4200-4207.

Breedveld, G.D., E. Pelletier, R. St Louis, G. Cornelissen, 2007, Sorption characteristics of polycyclic aromatic hydrocarbons in aluminum smelter residues, Environmental Science & Technology, 41(7), 2542-2547.

Chiou, C., T.D.E. Kile, 1998, Deviations from sorption linearity on soils of polar and nonpolar organic compounds at low relative concentrations, Environmental Science and Technology, 32(3), 338-343.

Durand, B., G. Nicaise, 1980, Procedures for Kerogen Isolation, Paris, Editions Technip.,

Endo, S.T., C. Schmidt, 2006, Prediction of partitioning between complex organic mixtures and water: Application of polyparameter linear free energy relationships, Environmental Science & Technology, 40(2), 536-545.

Gelinas, Y., K.M. Prentice, J.A. Baldock, J.I. Hedges, 2001, An improved thermal oxidation method for the quantification of soot/graphitic black carbon in sediments and soils, Environmental Science & Technology, 35(17), 3519-3525.

Ghosh, U., J.S. Gillette, R.G. Luthy, R.N. Zare, 2000, Microscale location, characterization, and association of polycyclic aromatic hydrocarbons on harbor sediment particles, Environmental Science and Technology, 34(9), 1729-1736.

Grathwohl, P., 1990, Influence of organic matter from soils and sediments from various origins on the sorption of some chlorinated aliphatic hydrocarbons. Implications on K_{OC} correlations, Environmental Science and Technology, 24(11), 1687-1693.

Gustafsson, O., F. Haghseta, C. Chan, J. MacFarlane, P.M. Gschwend, 1997, Quantification of the dilute sedimentary soot phase: Implications for PAH speciation and bioavailability, Environmental Science & Technology, 31(1), 203-209.

Huang, W.L., T.M. Young, M.A. Schlautman, H. Yu, W.J. Weber, 1997, A distributed reactivity model for sorption by soils and sediments .9. General isotherm nonlinearity and applicability of the dual reactive domain model, Environmental Science & Technology, 31(6), 1703-1710.

Jeong, S., M.M. Wander, S. Kleineidam, P. Grathwohl, B. Ligouis, C. J. Werth, 2008, The role of condensed carbonaceous materials on the sorption of hydrophobic organic contaminants in subsurface sediments, Environmental Science & Technology, 42(5), 1458-1464.

Jeong, S., C.J. Werth, 2005, Evaluation of methods to obtain geosorbent fractions enriched in carbonaceous materials that affect hydrophobic organic chemical sorption, Environmental Science & Technology, 39(9), 3279-3288.

Jonker, M.T.O., A. A. Koelmans, 2001, Polyoxymethylene solid phase extraction as a partitioning method for hydrophobic organic chemicals in sediment and soot, Environmental Science & Technology, 35(18), 3742-3748.

Jonker, M.T.O., A.A. Koelmans, 2002, Sorption of polycyclic aromatic hydrocarbons and polychlorinated biphenyls to soot and soot-like materials in the aqueous environment mechanistic considerations, Environmental Science & Technology, 36(17), 3725-3734.

Karapanagioti, H.K., S. Kleineidam, D.A. Sabatini, P. Grathwohl, B. Ligouis, 2000, Impacts of heterogeneous organic matter on phenanthrene sorption: Equilibrium and kinetic studies with aquifer material, Environmental Science & Technology, 34(3), 406-414.

Khalil, M.F., U. Ghosh, J.P. Kreitinger, 2006, Role of weathered coal tar pitch in the partitioning of polycyclic aromatic hydrocarbons in manufactured gas plant site sediments, Environmental Science & Technology, 40(18), 5681-5687.

Kleineidam, S., H. Rugner, B. Ligouis, P. Grathwohl, 1999, Organic matter facies and equilibrium sorption of phenanthrene, Environmental Science & Technology, 33(10), 1637-1644.

Kleineidam, S., C. Schuth, P. Grathwohl, 2002, Solubility-normalized combined adsorption-partitioning sorption isotherms for organic pollutants, Environmental Science & Technology, 36(21), 4689-4697.

Mahler, B. J., P.C. Van Metre, T.J. Bashara, J.T. Wilson, D.A. Johns, 2005, Parking lot sealcoat: An unrecognized source of urban polycyclic aromatic hydrocarbons, Environmental Science & Technology, 39(15), 5560-5566.

Pan, B., B.S. Xing, W.X. Liu, S. Tao, X.M. Lin, X.M. Zhang, Y.X. Zhang, Y. Xiao, H.C. Dai, H.S. Yuan, 2006, Distribution of sorbed phenanthrene and pyrene in different humic fractions of soils and importance of humin, Environmental Pollution, 143(1), 24-33.

Pignatello, J.J., B.S. Xing, 1996, Mechanisms of slow sorption of organic chemicals to natural particles, Environmental Science & Technology, 30(1), 1-11.

Ran, Y., K. Sun, X.X. Ma, G.H. Wang, P. Grathwohl, E.Y. Zeng, 2007a, Effect of condensed organic matter on solvent extraction and aqueous leaching of polycyclic aromatic hydrocarbons in soils and sediments, Environmental Pollution, 148(2), 529-538.

Ran, Y., K. Sun, Y. Yang, B.S. Xing, E. Zeng, 2007b, Strong sorption of phenanthrene by condensed organic matter in soils and sediments, Environmental Science & Technology, 41(11), 3952-3958.

Schwarzenbach, R.P., P.M. Gschwend, D.M. Imboden, 2003, Environmental Organic Chemistry, Hoboken, NJ, John Wiley & Sons, Inc.

Swift, R.S., D.L. Sparks, 1996, Organic Matter Characterization, Madison, Soil Sci. Soc. Am.

Wang, K.J., B.S. Xing, 2005, Chemical extractions affect the structure and phenanthrene sorption of soil humin, Environmental Science & Technology, 39(21), 8333-8340.

Xia, G.S., W.P. Ball, 1999, Adsorption-partitioning uptake of nine low-polarity organic chemicals on a natural sorbent, Environmental Science & Technology, 33(2), 262-269.

Xing, B.S., J.J. Pignatello, B. Gigliotti, 1996, Competitive sorption between atrazine and other organic compounds in soils and model sorbents, Environmental Science & Technology, 30(8), 2432-2440.

Appendix A.

Supporting Information for Chapter 2

Data Analysis

The input variables in our analysis include volume fractions of macerals in each sample (Table A1), density and OC contents (Table A2), and PAH concentrations of macerals or CMs (Table A3). Values were obtained from laboratory measurements or the literature. The uncertainty analysis was performed with Crystal Ball 2000 (Oracle Corp.) by assigning a uniform or normal distribution to each variable as defined in Table A4. The volume fractions of macerals in samples determined by organic petrography follow the normal distribution (*1*). The normal distribution was also assigned to the PAH concentrations in macerals by fitting the measured data in literature. The normality of the distribution was determined using the Anderson-Darling test and the Shapiro-Wilk test with Systat 12 (Systat Software, Inc.). The distribution of PAH concentrations in soot particles was changed to normal using a log-log transformation. Because there is very little information about the distributions of the density and OC contents of macerals, a uniform distribution was used (*2*, *3*).

Monte Carlo simulation was used to obtain the probability associated with the convolution of the input variables. Five hundred trials were sufficient to reach stable results. The resulting distributions were subjected to robust regression analysis of least trimmed squares with Systat 12. Means, standard deviations, and confidence levels of output parameters were obtained after eliminating the outliers.

Output parameters calculated from input variables include mass percentage and mass content of each CMs, OC contributed by CMs in samples, relative PAH contribution from CMs, and potential PAH loading on coal tar. Equations used to calculate these parameters are listed in Table A5. The remaining table (A6) and figures (A1-A4) are referred to in the text of Chapter 2.

Table A1. Maceral groups and their subgroups quantified with petrographic analysis.

QUANTITATIVE MICROSCOPICAL ANALYSIS

Location: Lake Como, Lake Fosdic (Texas) | **Lithology:** lake sediments, soils, street dusts, parking dusts | **Composition** (Vol. %, 500 points counted on two polished mounts)

Preparation: polished mount of organic concentrate (after acid treatment, no crushing) | **Sample :**

	Maceral group	Maceral subgroup / Maceral	Reflected light (oil immersion)	Fluorescence (uv-light + violet-light excitation; oil immersion)	LS 0 5	LS 10 - 15	LS 25 30	IBS infl. b. s.	LFS Fosdic	CS com. soil	RS resid. s.	RSD street d.	UPD unseal.p.	SPD sealed p.
Recent organic matter (soil, peat, lake sediment...) and Organic matter in ancient sediments	Huminite	Telohuminite	fragments (10-700 µm) of ungelified or partly gelified tissues (stems, roots) reddish-brown and middle grey	dark-brown to orange-brown	3.8	2.4	5.3	29.7	29.0	54.4	33.9	23.6	13.4	4.3
		Detrohuminite	fine humic detritus (<10 µm) that may be cemented by amorphous humic matter	dark-brown to non-fluorescing	50.4	54.5	56.3	10.7	29.0	8.7	31.0	2.6	4.3	0.2
		Gelohuminite	amorphous humic gel (gelinite) and cell excretions (corpohuminite)	dark-brown to non-fluorescing	1.8	0.8	0.8	3.5	3.7	5.3	5.5	4.8	3.1	1.0
	Vitrinite	Telovitrinite	/											
		Detrovitrinite	isolated fragmentary particles of gelified tissues, homogeneous, middle grey to light grey (wide range of reflectance), equidimentional, 2 to 10 µm; most of them are monomaceral coal particles (vitrite)	non-fluorescing	0.6	0.6	1.2	0.4	0.4	0.2	x			
		Gelovitrinite	/											
	Liptinite	Sporinite	orange-brown to dark grey microspores (spores, pollen)	moderately intense to intense, yellow-brown, yellow	1.6	3.0	2.6	0.6	2.3	1.2	0.3			
		Cutinite	orange-brown to dark grey fragments of cuticles	moderately intense to intense, yellow-brown, yellow	0.2	0.2	x	1.8	2.5	1.7	x	4.9	1.2	
		Fluorinite	small intra-cellular granules in fragments of leaf tissues (lipid secretions)	moderately intense to intense, yellow-green, yellow	x				x					
		Suberinite	fragments of tissues (25 to 300 µm), orange-brown; bark-or cork-derived tissues	intense green and yellow-green	0.4	0.6	1.0	2.3	0.8	0.7	0.8	2.8		0.2
		Resinite	intra-/extra-cellular resin bodies, terpene resinites	intense yellow, green		0.2	0.2	2.9	3.7	0.7		4.5	2.1	0.2
		Chlorophyllinite	occurs sporadically as small particles (1-5 µm)	intense blood-red					x					
		Telalginite	/											
		Lamalginite	/											
		Liptodetrinite	small fragments of liptinites less than 10 µm in size; occurs associated with detrohuminite	moderately intense to intense, yellowish-brown to yellow	8.7	17.9	7.4	0.4	6.2	0.2	6.3		0.3	
		Bituminite: AOM												
		- orange-brown	/											
		- gray to gray-brown	/											
		- orange-brown matrix	/											
		Migrabitumen: non-fluorescing	/											
		Oil inclusions	/											
		Oil expulsions	/											
	Inertinite	Fusinite	high reflecting, white tissues (degradofusinite), 10 to 300 µm		x		0.2	x	0.2	0.7	x	x		
		Semifusinite	low reflecting, light-grey tissues: oxysemifusinite (dehydratation/oxidation), degradosemifusinite (biodegradation), 10 to 200 µm					x		x				x
		Funginite	middle grey to light grey sclerotia, single or multi-celled fungal spores, hyphae and other fungal remains		x	x	x	0.2	0.2	1.0	1.3	0.6	x	
		Secretinite	/											
		Macrinite	/											
		Micrinite	/											
		Inertodetrinite	isolated fragmentary particles of semifusinite and fusinite: homogeneous, light grey to white, equidimentional, 2/4 to 10 µm		0.8	0.2	0.6	0.2	0.4	1.0	0.3			
	Natural coke		/											
	Natural char		/											
Anthropogenic contamination	Hard coal	Sub-bituminous coal			0.2		0.4			x				
		High-volatile bit. coal	low coal particles are strongly weathered and show oxidation rims		x		x		x	0.2	x			
		Medium-volatile bit. coal	/											
		Low-volatile bit. coal	/											
		Anthracite	contains pyrite, some particles are weathered					x			0.2			0.6
	Coke (coal carbonization)		subrounded to angular carbon particles showing a wide range of microstructures (porosity, pore sizes and shapes, cell-wall thicknesses) and microtexturas identified by anisotropy, shape and size of domains		0.2	x	0.2	0.2	0.2	x	0.2	x	x	0.2
	Char (mostly from coal combustion)		spheroidal carbon particles with vesicles, more or less porous and anisotropic, mostly high reflecting: thin-walled cenospheres (tenuispheres), thick-walled cenospheres (crassispheres)		x	0.2	x	x	x	x	x			x
	Soot (traffic, oil combustion)		subangular carbon particles with grainy texture, mostly isotropic, more or less porous, yellowish-grey to white or blue-grey, heterogeneous reflectance; some with cracks	blue-grey soot : dark brown; greenish films of hydrocarbons are often generated during the fluorescence excitation; grey, white soot : non-fluorescing	15.8	13.8	16.5	7.4	9.0	5.0	3.4	8.5	13.1	5.0
	Coal- and Petroleum- derived fluorescent materials (tar, oils, lubricants...)		dark grey, reddish-brown, dark brown, sticky, subangular asphalt-like particles, presence of scratches (softness of the material), some with peripherical differentiation (darker), pores, granular surface, cracks	moderately intense reddish-brown, dark brown	5.2	1.4	1.3	9.5	4.3	1.8	10.8	32.9	45.3	26.4
			dark brown or black bitumen-like substances occuring as sticky irregular bodies and droplets; some are multivacuolate (gas bubbles?) or show flow structure or network texture (in fluorescence); often yellow-green fluorescing oil drops and oil films partly covering the bitumen-like substances	moderately intense to intense brown-yellow, orange-brown; high yellow fluorescence of the embedding resin in contact with the bitumen (resin acts as a chemical extractor)	7.1	4.2	5.6	28.8	8.1	13.7	6.0	14.8	9.5	4.9
			coal tar pitch: more or less fine granular, grey, grey-brown, some with scratches, contains often thin anisotropic coke particles and cenospheres	non-fluorescing or expulsion of green fluorescing hydrocarbons under UV irradiation; high yellow-orange fluorescence of the embedding resin in contact with the pitch particles (resin acts as a chemical extractor)	3.2	x	0.4	1.4	x	3.5	x		7.7	57.0

Note that concerning the huminite group and vitrinite group, the table shows only the maceral subgroups. AOM: Amorphous Organic Matter. x : present but not expressed as percentage due to scarcity
Other encountered materials: plastics (samples IBS, RSD, UPD, SPD), paint particles (UPD), metals (samples IBS, LFS, CS, RSD, UPD, SPD)

Table A2. Densities and OC contents of maceral groups reported in literature or measured in our laboratory.

Maceral Group	Density (g/cm^3)	OC Content (wt %)
Huminite[a]	1.12 (4)	60-77 (5)
Vitrinite	1.28-1.70 (6)	70.5-96 (1, 7)
Liptinite	1.10-1.22 (6)	83 - 89 (8)
Inertinite	1.30-1.45 (4)	71.0–94.0 (9)
Hard Coal	Bituminous coal:1.15-1.7 (4); Anthracite coal:1.32-1.80 (4)	85.2-96.4 (10)
Coke	1.6-1.8 (11)	87-89 (1)
Char	0.1-1.0 (12)	66-87 (13)
Soot	1.22-1.82 (10)	32.2-77.0 (10, 14)
Asphalt- and bitumen-like substances[a, b]	1.07	84.1-84.7
Coal-tar pitch[a, b]	1.16	62.4-63.1

a. Closely spaced values above and below the point value (i.e., within 0.0001%) were used as the lower and upper limits of a uniform distribution to meet the functional requirement of Crystal Ball
b. Data were measured in our laboratory with commercial asphalt and coal-tar sealant which are similar to the product used in sampling sites.

Table A3. The sum of 11 PAHs in CMs reported in literature or measured in our laboratory (phenanthrene, anthracene, fluoranthene, pyrene, benz(a)anthracene, chrysene, benzo[b]fluoranthene, benzo[k]fluoranthene, benzo(a)pyrene, indeno[1,2,3-cd]pyrene, and benzo[ghi]perylene).

CM Particles	Total PAHs[a] (mg/kg)	Standard Deviation
Recent OM[a]	68	33
Coal[b]	620	400
Coke[b]	510	270
Char/charcoal[c]	44	NA[e]
Soot[d]	85	5.3
Asphalt[a]	2,850	160
Coal-tar pitch[a]	75,000	21,700

a. Recent OM, asphalt, and coal-tar pitch were separated from samples and PAHs were measured in our laboratory.
b. Coal and coke particles were separated from coke oven site soil(*15*).
c. Char/charcoal particles were from combustion of bark (*10*).
d. Soot samples were collected from vehicle exhaust pipes, including gasoline and diesel soot (*16*), and the mean and standard deviation of log-log-transformed data were used.
e. NA: not available

Table A4. Assigned probability distribution of input variables used in Crystal Ball.

Assumption Cells	Probability Distribution
Volume fraction (%)	Normal distribution[a]
Density of macerals (g/cm^3)	Uniform distribution
Organic carbon (OC) content of macerals (g/100g)	Uniform distribution
PAHs in macerals (mg/kg)	Normal distribution[b]

a. Mean was determined by petrographic analysis (Table A1), and the standard deviation was obtained by interpolating the correlation between mean and standard deviation of maceral counts of duplicate samples in literature (*17*), $Standard\ \ Deviation = 0.30 \times Mean^{0.51}$.

b. Mean and standard deviation of normal distribution were obtained through our measurement or literature data (Table A3) except soot and char/charcoal. The log-log-transformed values of PAHs in soot were assigned to follow the normal distribution. The Uniform distribution was assigned to PAHs in char/charcoal because of the limit of data.

Table A5. Forecasting cells (output parameters) with equations defined in Crystal Ball.

Forecasting cells	Equations
Mass percentage of CM_i (%)	$Mass\ Percentage\ of\ CM_i = \frac{Volume\ Percentage\ of\ CM_i \times Density\ of\ CM_i}{\sum_i (Volume\ Percentage\ of\ CM_i \times Density\ of\ CM_i)} \times 100\%$
Mass content of CMi (g CMi / 100g bulk sample)	$Mass\ Content\ of\ CM_i\ in\ Sample = Mass\ Percentage\ of\ CM_i \times Total\ CM\ in\ Sample$
OC from CM_i in each sample (g OC / 100 g bulk sample)	$OC\ Contributed\ by\ CM_i = \frac{Mass\ Percentage\ of\ CM_i \times OC\ Content\ of\ CM_i}{\sum_i (Mass\ Percentage\ of\ CM_i \times OC\ Content\ of\ CM_i)} \times TOC\ of\ Bulk\ Sample$
Percent of PAHs distributed in CM_i in each sample (%)	$PAHs\ in\ CM_i(\%) = \frac{Mass\ Percentage\ of\ CM_i \times PAHs\ in\ CM_i}{\sum_i (Mass\ Percentage\ of\ CM_i \times PAHs\ in\ CM_i)} \times 100\%$
Potential PAH loadings from coal tar pitch in each sample (mg PAHs / kg bulk sample)	$Potential\ PAHs\ from\ Pitch = PAHs\ in\ Pitch\ Particles \times Mass\ Content\ of\ Pitch\ in\ Sample$

Table A6. Correlation coefficients between total PAHs and OC contents in different CMs ($\log(\sum_{13}\mathrm{PAH}) = ax + b$).

x		a	b	R^2
OC in coal tar, asphalt, and soot (%)	With RS and RSD	0.80	2.74	0.66
	Without RS and RSD	0.71	3.14	0.96
OC in coal tar, asphalt, and soot (%)	HMW PAHs	0.71	3.08	0.96
	LMW PAHs	0.69	2.37	0.95

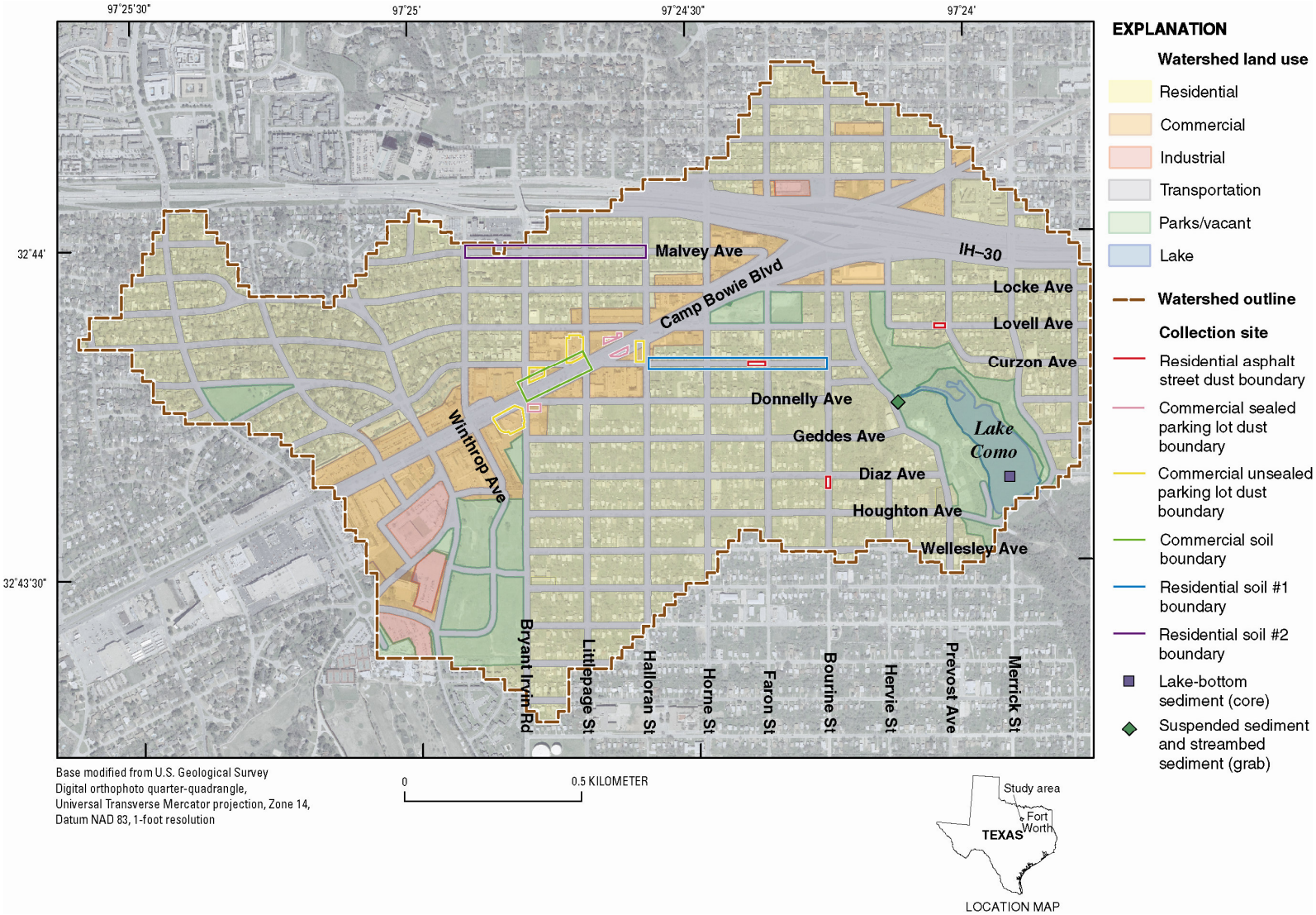

Figure A1. Sites where samples were collected in Lake Como watershed, Fort Worth, Texas (*18*).

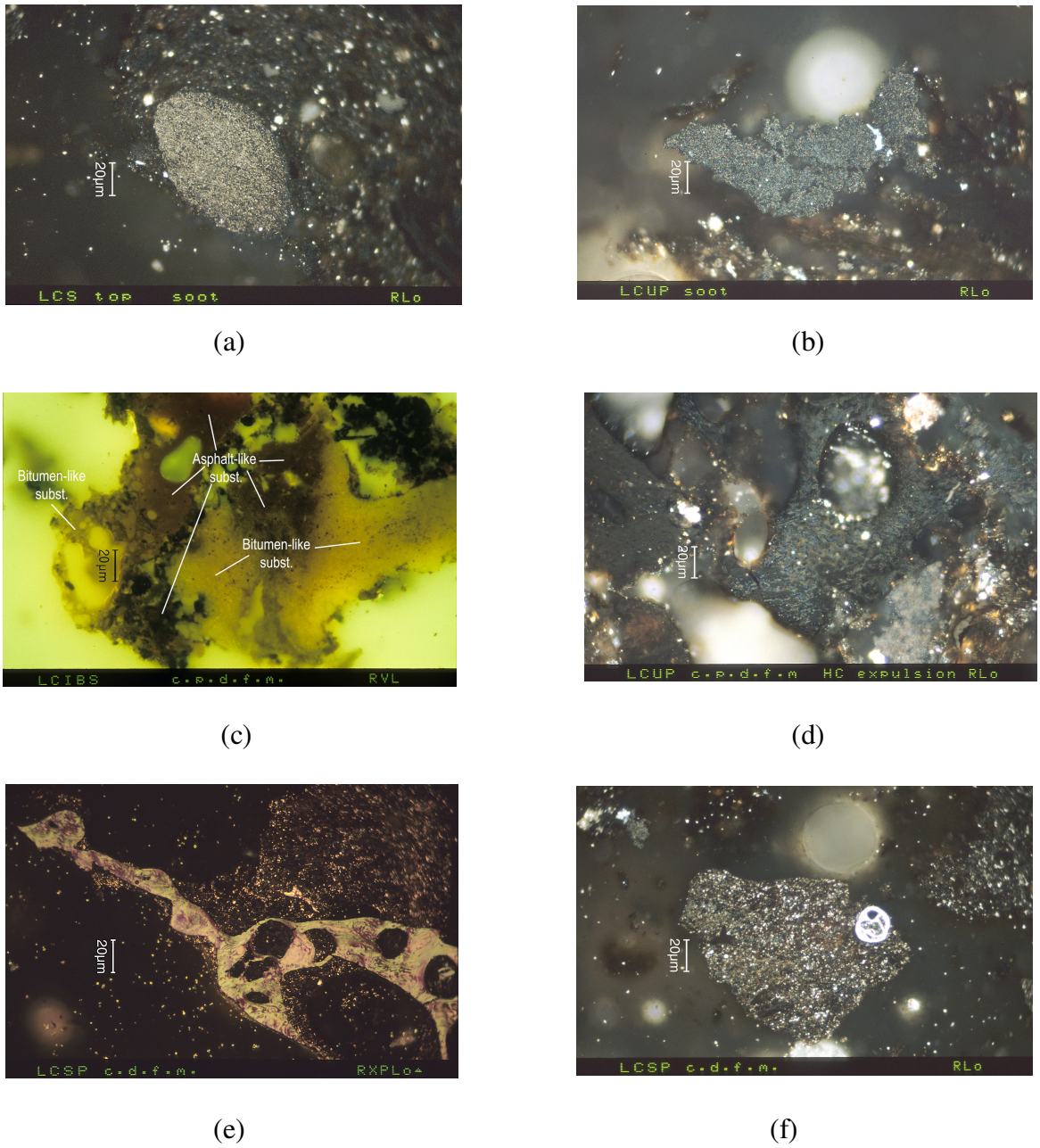

Figure A2. Photomicrographs illustrating the different CMs present in the selected Lake Como watershed samples: (a) rounded soot particle from top sediment of 0-5 cm; (b) porous blue grey soot from unsealed parking lot dust; (c) asphalt-like substances and bitumen-like substances from streambed sediment. Note the flow srtucture with bubbles and the bright yellow exsudates; (d) asphalt with large vesicles from unsealed parking lot dust; (e) coal tar pitch (right above corner) containing a coke particle showing large pores from sealed parking lot dust; (f)coal tar pitch embedding a cenosphere (multi-celled body) from sealed parking lot dust (Note than (a), (b), (d), and (f) used white reflected light and oil immersion; (c) used fluorescence mode and oil immersion; (e) used obliquely crossed polars, lambda plate, oil immersion) .

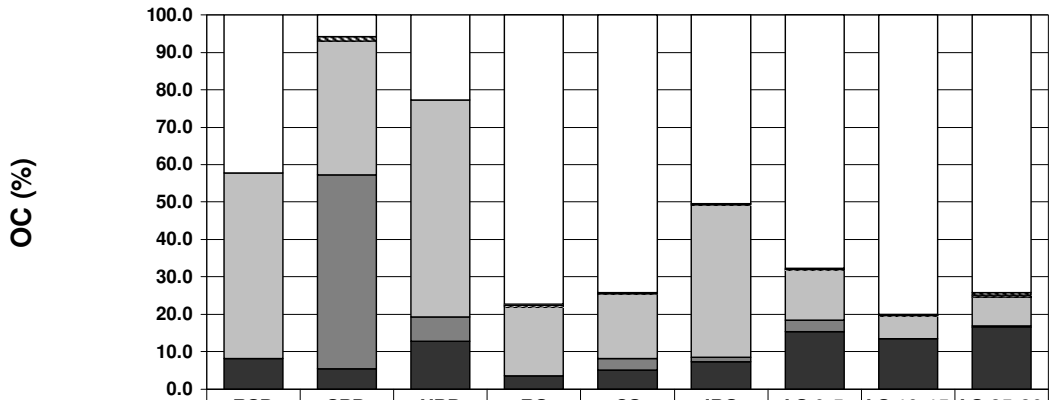

	RSD	SPD	UPD	RS	CS	IBS	LS 0-5	LS 10-15	LS 25-30
Recent OM	42.4	5.8	22.8	77.3	74.1	50.3	67.5	80.2	74.4
Hard Coal	0.0	1.0	0.0	0.3	0.4	0.0	0.3	0.0	0.6
Char	0.0	0.0	0.0	0.0	0.0	0.0	0.0	0.0	0.0
Coke	0.0	0.4	0.0	0.4	0.0	0.4	0.4	0.1	0.4
Asphalt- and Bitumen-like Substances	49.6	35.6	58.0	18.6	17.4	40.9	13.4	6.1	7.6
Coal-Tar Pitch	0.0	52.1	6.6	0.0	3.2	1.2	2.8	0.0	0.4
Soot	8.0	5.2	12.6	3.4	5.0	7.3	15.5	13.6	16.6

Figure A3. Distribution of OC among CMs in Lake Como watershed samples.

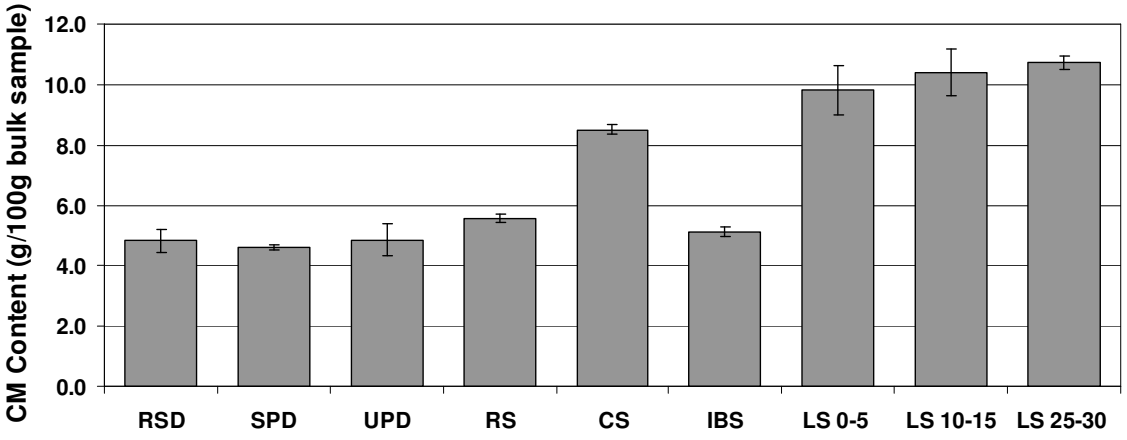

Figure A4. Total CM contents in Lake Como watershed samples (error bars represent ±1 standard deviation).

References

(1) Taylor, G.H., M. Teichmuller, A. Davis, C.F.K. Diessel, R. Littke, P. Robert, 1998, Organic Petrology, Berlin, Gebrüder Borntraeger.

(2) Rodger, C., J. Petch, 1999, Uncertainty & Risk Analysis, Business Dynamics, PricewaterhouseCoopers: United Kingdom firm.

(3) Ferson, S., L. Ginzburg, R. Akçakaya, 1997, Whereof one cannot speak: When input distributions are unknown, Risk Analysis, http://www.ramas.com/whereof.pdf.

(4) Tyson, R.V., 1995, Sedimentary Organic Matter. Organic Facies and Palynofacies. Chapman & Hall, London.

(5) Sykorova, I., W. Pickel, K. Christanis, M. Wolf, G.H. Taylor, D. Flores, 1994, Classification of huminite - ICCP system, International Journal of Coal Geology, 62, 85-106.

(6) Dormans, H.N.M., F.J. Huntjens, D.W. Van Krevelen, 1957, Chemical structure and properties of coal - composition of the individual macerals (vitrinites, fusinites, micrinites and exinites), Fuel, 321-339.

(7) ICCP, The new vitrinite classification (ICCP System 1994), 1998, Fuel, 77, 349-358.

(8) Ward, C.R., L.W. Gurba, 1999, Chemical composition of macerals in bituminous coals of the Gunnedah Basin, Australia, using electron microprobe analysis techniques, International Journal of Coal Geology, 39, 279-300.

(9) ICCP, The new inertinite classification (ICCP System 1994), 2001, Fuel, 80, 459-471.

(10) Jonker, M.T.O., S.B. Hawthorne, A.A., Koelmans, 2005, Extremely slowly desorbing polycyclic aromatic hydrocarbons from soot and soot-like materials: Evidence by supercritical fluid extraction, Environmental Science & Technology, 39, 7889-7895.

(11) Ahn, S., D. Werner, H.K., Karapanagioti, D.R. McGlothlin, R.N. Zare, R.G. Luthy, 2005, Phenanthrene and pyrene sorption and intraparticle diffusion in polyoxymethylene, coke, and activated carbon, Environmental Science & Technology, 39, 6516-6526.

(12) Byrne, C.E., D.C. Nagle, 1997, Carbonization of wood for advanced materials applications, Carbon, 35, 259-266.

(13) Goldberg, E.D., 1985, Black Carbon in the Environment: Properties and Distribution. A Wiley-Interscience Publication: John Wiley & Sons: New York.

(14) Bucheli, T.D., O. Gustafsson, 2000, Quantification of the soot-water distribution coefficient of PAHs provides mechanistic basis for enhanced sorption observations, Environmental Science & Technology**,** 34, 5144-5151.

(15) Ahn, S., D. Werner, R.G. Luthy, 2005, Physicochemical characterization of coke-plant soil for the assessment of polycyclic aromatic hydrocarbon availability and the feasibility of phytoremediation, Environmental Toxicology and Chemistry, 24, 2185-2195.

(16) Boonyatumanond, R., M. Murakami, G. Wattayakorn, A. Togo, H. Takada, 2007, Sources of polycyclic aromatic hydrocarbons (PAHs) in street dust in a tropical Asian mega-city, Bangkok, Thailand, Science of the Total Environment, 384, 420-432.

(17) Wild, G.D., K.W., Kuehn, J.C., Hower, 2000, Assessment of compositional variation in duplicate samples of pelletized coal, International Journal of Coal Geology, 42, 231-240.

(18) Wilson, J.T., P.C. Van Metre, C.J. Werth, Y. Yang, 2006, Particle-associated contaminants in street dust, parking lot dust, soil, lake- bottom sediment, and suspended and streambed sediment, Lake Como and Fosdic Lake watersheds, Fort Worth, Texas, 2004 U.S. Geological Survey Data Series 211. Denver, CO, U.S. Geological Survey http://pubs.usgs.gov/ds/2006/211/ (accessed May 2009), 24pp.

Appendix B.

Supporting Information for Chapter 3

The equations to estimate the TOC determined by organic petrography are listed in Table B1, and the TOC estimated by petrography is compared to that measured by elemental analysis in Figure B2. The mass loss of asphalt and coal tar after each step of chemical treatment used in Cr_2O_7 oxidation is presented in Figure B1. Table B2 shows the chemical characteristics of reference asphalt and coal tar materials and the BC contents determined in these reference materials by Cr_2O_7 Oxidation and CTO-375. Tables (B1 and B2) and figures (B1 and B2) are referred to in the text of Chapter 3.

Table B1. Equations to estimate the TOC determined by organic petrography.

Forecasting cells	Equations	
Mass percentage of CM_i (%)	$Mass\ Percentage\ of\ CM_i = \frac{Volume\ Percentage\ of\ CM_i \times Density\ of\ CM_i}{\sum_i (Volume\ Percentage\ of\ CM_i \times Density\ of\ CM_i)} \times 100\%$	(1)
Mass content of CMi (g CMi / kg bulk sample)	$Mass\ Content\ of\ CM_i\ in\ Sample = Mass\ Percentage\ of\ CM_i \times Total\ CM\ in\ Sample$	(2)
OC from CM_i in each sample (g OC / kg bulk sample)	$OC\ Contributed\ by\ CM_i = Mass\ Content\ of\ CM_i \times OC\ Content\ of\ CM_i$	(3)
TOC (g OC / kg bulk sample)	$TOC = \sum_i OC\ Contributed\ by\ CM_i$	(4)

Table B2. Chemical characteristics of reference asphalt and coal tar materials and their BC contents determined by Cr_2O_7 Oxidation and CTO-375.

	OC(g/kg)	H/C	BC by Cr_2O_7			BC by CTO-375		
			BC (g/kg)	H/C	BC/OC	BC(g/kg)	H/C	BC/OC
Commercial Asphalt	844.3±4.2	0.13	727.2±0.2	0.12	0.86	ND*	ND	ND
Commercial Coal Tar	627.6±4.8	0.06	244.7±1.7	0.05	0.39	71.8±1.5	0.04	0.11
Picked Asphalt Particles	834.3±31.2	0.08	ND	ND	ND	ND	ND	ND
Picked Coal Tar Particles	572.2±5.8	0.06	ND	ND	ND	69.2*	0.02	0.12

* ND: not detected

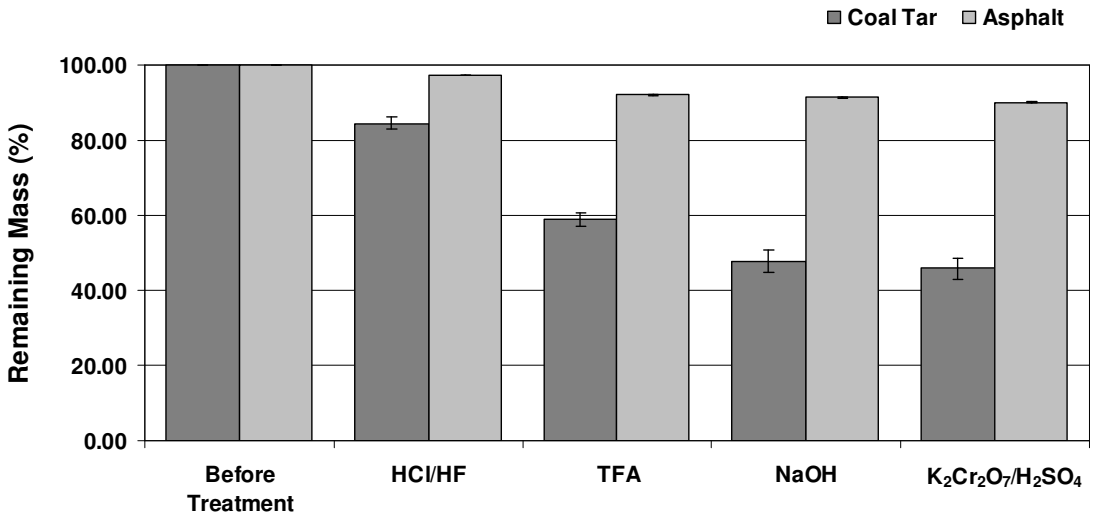

Figure B1. The mass loss of asphalt and coal tar after each step of chemical treatment used in Cr_2O_7 oxidation.

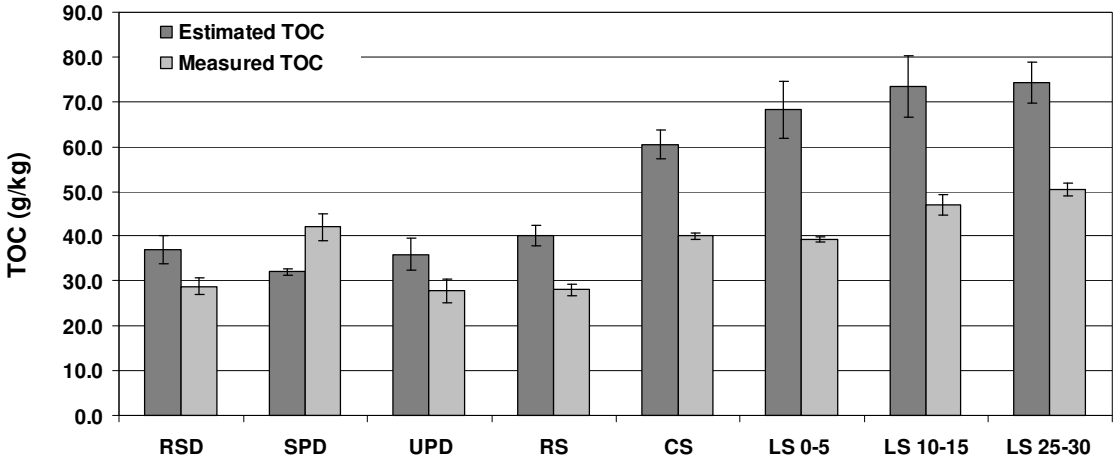

Figure B2. Comparison of petrography-estimated TOC to measured TOC in Lake Como watershed samples of residential street dust (RSD), sealed parking lot dust (SPD), unsealed parking lot dust (UPD), residential soil (RS), commercial soil (CS), lake sediment from 0-5 cm depth (LS 0-5), lake sediment from 10-15 cm depth (LS 15-20), and lake sediment from 25-30 cm depth (LS 25-30).

Appendix C.

PAH Distribution and Sorption to Density-separated Fractions of Urban Dust, Soils, and Sediments in Fosdic Lake Watershed, Fort Worth, Texas

C.1 Sample Collection

Samples of urban dust, soil, and lake sediment were collected from the Fosdic Lake watershed in Fort Worth, Texas, at the same time when Lake Como watershed samples were collected. Fosdic Lake watershed samples include residential street dust (F-RSD), sealed parking lot dust (F-SPD), unsealed parking lot dust (F-UPD), soil from residential area (F-RS), soil from commercial area (F-CS), and three Fosdic Lake sediments (depths from the top: 0-5 cm, 15-20 cm, and 25-30 cm) (F-LS1, F-LS2, and F-LS3). Sample collection and preparation methods were the same as described in Chapter 2 for Lake Como watershed samples. Details of the sampling sites (Figure C1) and methods are presented in Wilson et al. (*1*).

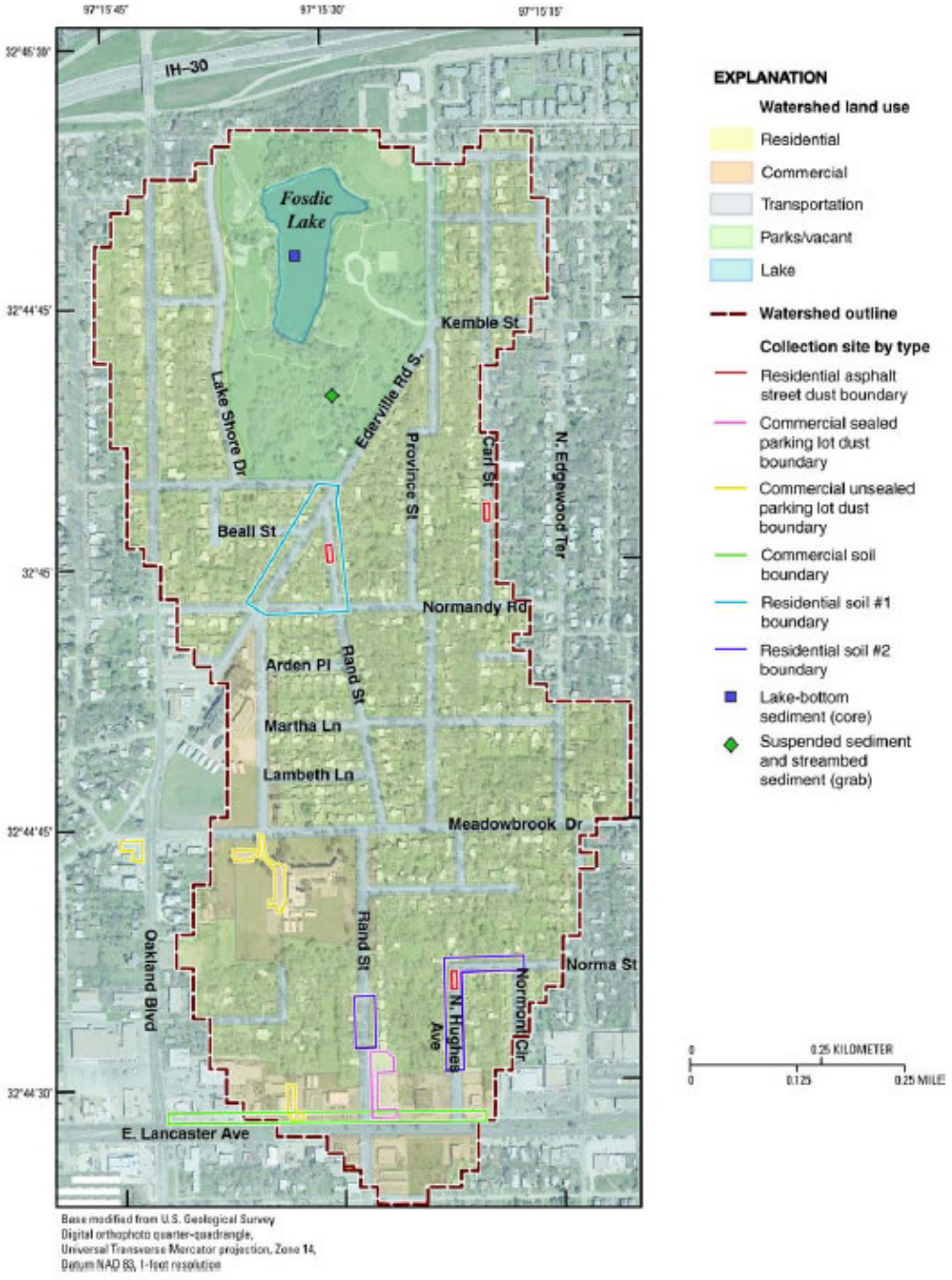

Figure C1. Sites where samples were collected in Fosdic Lake watershed, Fort Worth, Texas (*1*).

C.2 Density Separation

Representative sub-samples of Fosdic Lake watershed samples were separated into light (LFr) and heavy (HFr) fractions with a solution of 1.60 g/cm^3 sodium polytungstate as described in Chapter 3. Same as Lake Como watershed samples, the majority of mass is associated with HFr fractions, ranging from 92.1% to 99.6% (Figure C2).

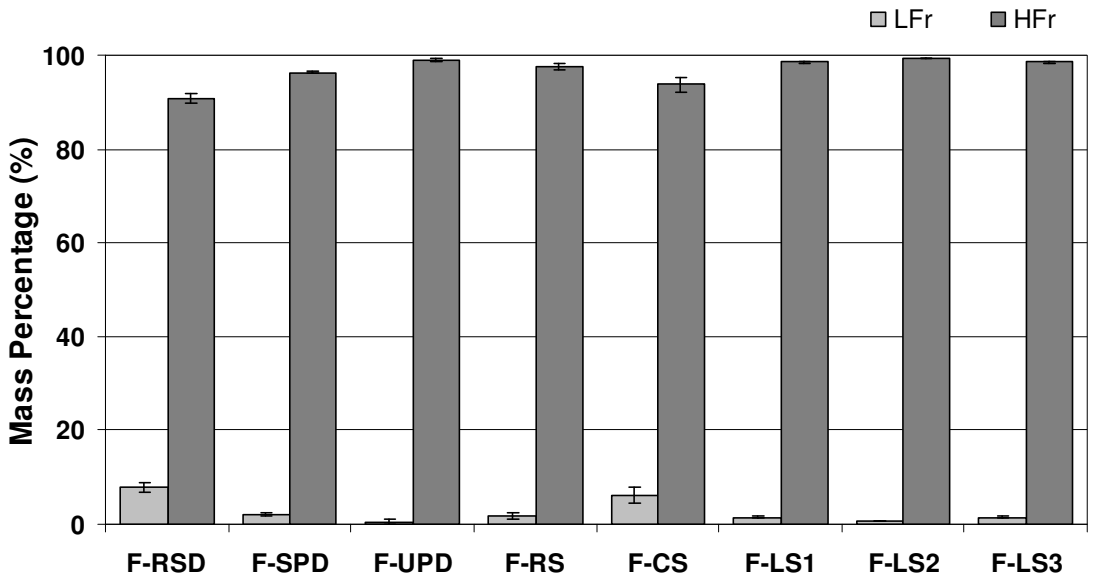

Figure C2. Mass percentages of LFr and HFr fractions of Fosdic Lake watershed samples.

C.3 Carbon Analysis

Organic carbon (OC) contents of bulk samples and LFr and HFr fractions were determined with a CE 440 CHN analyzer (Exeter Analytical, Inc.) in the Microanalysis Laboratory at UIUC after the removal of inorganic carbon. Although OC contents in LFr fractions are 4 to 22 times higher than those in HFr fractions (Table C1), the majority of

OC is associated with HFr fractions in all samples except in the sample F-RSD (Figure C3).

Table C1. OC contents in bulk samples and LFr and HFr fractions of Fosdic Lake watershed samples.

OC (%)	F-RSD	F-SPD	F-UPD	F-RS	F-CS	F-LS1	F-LS2	F-LS3
Bulk	3.36	4.04	1.56	3.92	4.68	8.29	7.15	7.02
LFr	30.09	44.34	33.76	27.96	24.86	35.87	30.11	32.32
HFr	1.35	3.84	1.64	2.21	3.73	7.87	6.86	7.82

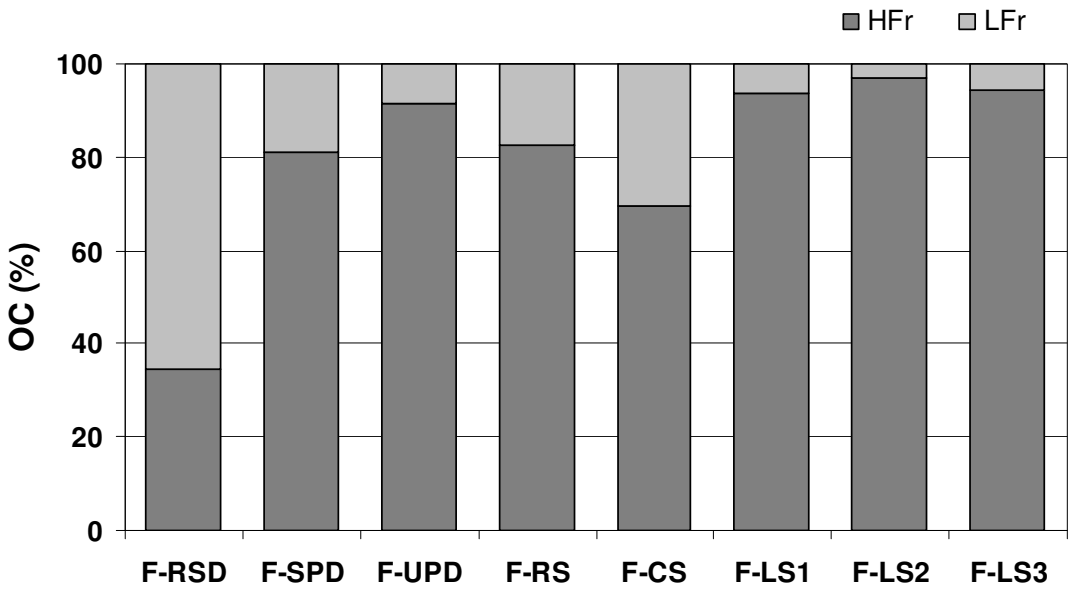

Figure C3. The distribution of OC between LFr and HFr fractions of Fosdic Lake watershed samples.

C.4 PAH Analysis

Eighteen parent PAHs, nine specific alkyl-PAHs, and the homologous series of alkyl-PAHs in bulk samples were determined at the USGS laboratory as described in Chapter 2. The sum of 13 consensus-based sediment-quality-guideline (SQG) PAHs in bulk samples are reported to compare with the probable effect concentration (PEC) and the threshold effect concentration (TEC) (*2*) (Figure C4).

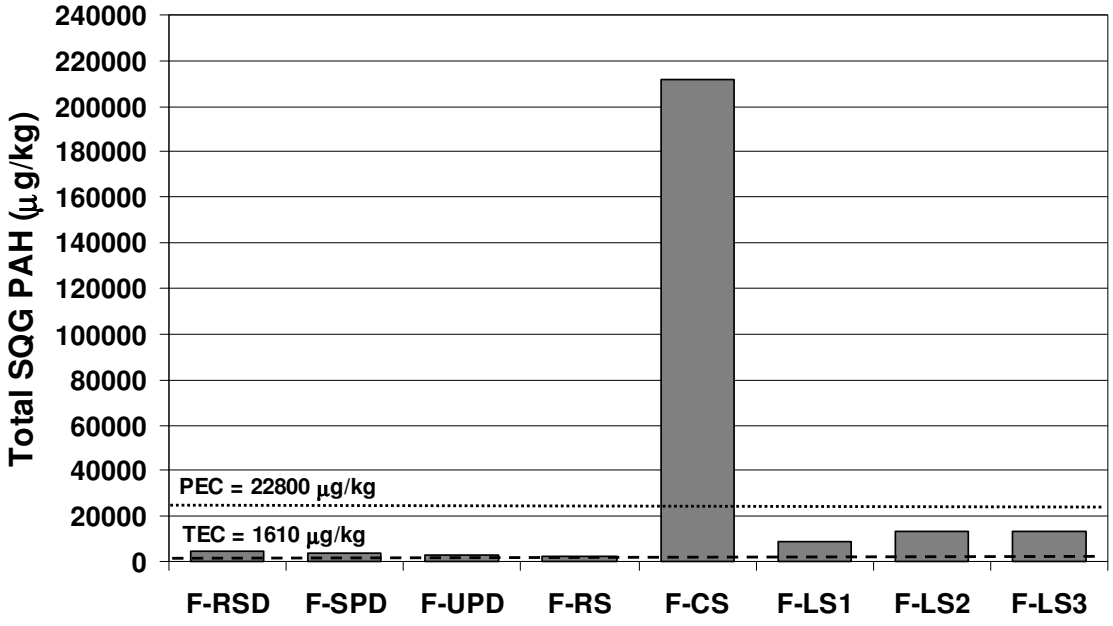

Figure C4. Total SQG PAHs in Fosdic Lake watershed samples.

Density-separated LFr and HFr fractions were extracted with acetone and dichromathane by accelerated solvent extraction (ASE) at UIUC (EPA method 3545). The extract was cleaned with silica gel (EPA method 3630c), and 16 EPA priority PAHs were analyzed with GC/MS following EPA method 8270c. The sum of 16 EPA PAHs was reported as total PAHs for LFr and HFr fractions. Except for the sample F-CS, the total of 16 PAHs are 4-27 times higher in LFr fractions than in HFr fractions due to the

higher OC contents in LFr fractions (Figure C5). However, most PAHs are associated with HFr fractions (>65%) in all samples (Figure C6). This can be attributed to the dominant mass (>92%) and dominant OC content (>70%) in HFr fractions for most samples (Figure C2 and C3). Our results are different from what was observed in two estuarial sediments from NY/NJ Harbor by Rockne et al. (*3*). In their study, 54% and 85% of PAHs were associated with low density fractions that represent 15% and 3.6% of total sediment mass, and 22% and 34% of total OC mass. This suggests that not only the amount of CMs but also the type, properties, and sorption capacity of CMs determine the distribution of PAHs. It is expected that CMs in urban watershed samples and estuarial harbor sediments are different in compositions and properties because they come from different source materials and age under different environmental conditions. The source-determined PAH compositions play an import role as well. These may also be the reasons that more than 75% of PAHs are associated with HFr of residential street dust which represents less than 35% of total OC in the sample (Figure C3 and C6).

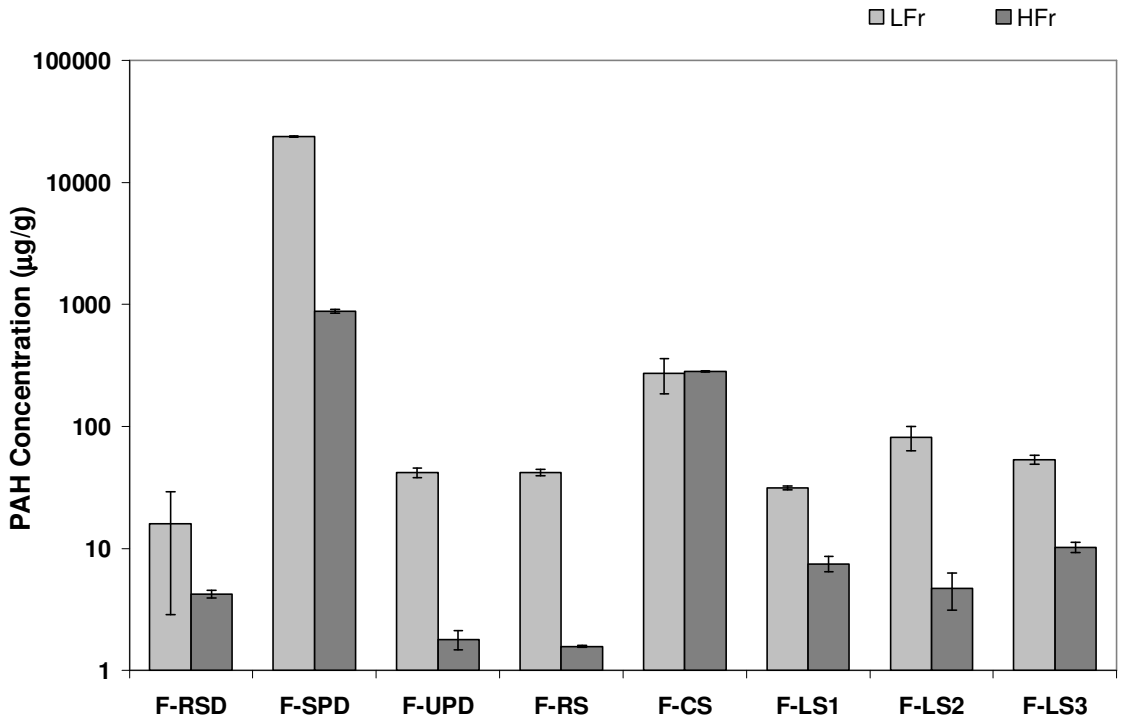

Figure C5. Concentrations of 16 EPA PAHs in LFr and HFr fractions of Fosdic Lake watershed samples.

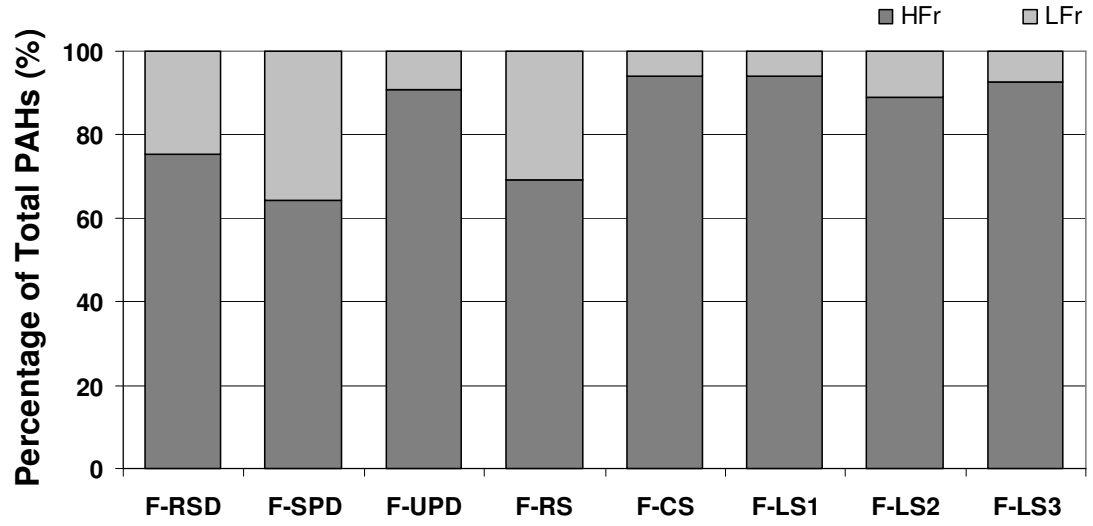

Figure C6. Distribution of 16 EPA PAHs in LFr and HFr fraction of Fosdic Lake watershed samples.

C.5 Phenanthrene Sorption Measurement

Sorption isotherms were measured using established batch equilibrium methods with ^{14}C-phenanthrene as the sorbate and LFr and HFr fractions as sorbents. Experiment details were given in Chapter 4. The sorption data were fit with both the Freudnlich isotherm model (Eq 1) and the linear partitioning model (Eq 2):

$$logC_S = logK_F + N\ logC_W \quad \text{(Eq 1)}$$

$$C_S = K_D C_W \quad \text{(Eq 2)}$$

where C_S is the solid-phase concentration (μg/kg) and C_W is the aqueous concentration (μg/L); K_F is the Freundlich solid-water distribution coefficient [(μg/kg)/(μg/L)^N]; K_D is the linear solid-water partition coefficient (L/kg); and N is the Freundlich exponent.

The OC normalized partitioning coefficient (K_{OC}) was calculated with Eq 3:

$$K_{OC} = \frac{K_D}{f_{OC}} \quad \text{(Eq 3)}$$

The relative contributions of HFr and LFr fractions to phenanthrene sorption were calculated using:

$$Relative\ \ Sorption\ \ Contribution\ \ of\ \ Fraction\ \ i = \frac{C_{S,i}}{\Sigma C_{S,i}} \times 100\% \quad \text{(Eq 4)}$$

Similar to samples from Lake Como watershed, sorption isotherms for samples from Fosdic Lake watershed are all nearly linear (N >0.90, Table C2). The $logK_{oc}$ values of HFr fractions are higher than those of LFr fractions, with the greatest difference in the sample F-RSD. It is reasonable to assume that more condensed CMs which have stronger sorption capacity are associated with HFr than with LFr in our samples even though further verification is still needed. In contrast, Rockne et al. (*3*) reported that $logK_{oc}$

Table C2. Sorption isotherm parameters of LFr and HFr fractions of Fosdic Lake watershed samples.

Sample ID	Fraction	$logK_F$ $(\mu g/kg)/(\mu g/L)^N$	N	$logK_D$ (L/kg)	log Koc (L/kg C)
F-RSD	LFr	3.91	0.95	3.76	4.28
	HFr	3.24	0.91	2.99	4.86
F-SPD	LFr	4.18	0.99	4.10	4.46
	HFr	3.47	0.94	3.24	4.65
F-UPD	LFr	4.09	0.99	3.99	4.46
	HFr	3.35	0.90	3.03	4.81
F-RS	LFr	3.95	0.95	3.91	4.46
	HFr	3.17	0.92	2.99	4.65
F-CS	LFr	3.93	0.95	3.79	4.40
	HFr	3.32	0.93	3.14	4.57
F-LS1	LFr	3.88	0.99	3.83	4.28
	HFr	3.34	0.97	3.34	4.44
F-LS2	LFr	3.90	0.98	3.92	4.44
	HFr	3.47	0.99	3.45	4.61
F-LS3	LFr	3.84	0.99	3.92	4.41
	HFr	3.42	0.95	3.33	4.44

values of low density fractions were approximately 10 times higher than those of high density fractions in their estuarial sediment samples. Although the results of our study are different from those of Rockne et al.(*3*), the conclusion is the same that the majority of native PAHs are associated with the fraction of CMs that have higher sorption capacity. In our results, this fraction is the HFr fraction (Figure C7). HFr fractions dominate sorption with contributions of more than 67%. This suggests that redistribution of PAHs between LFr and HFr is not likely, and HFr fractions concentrate, transport, and retain

the majority of total PAHs in urban watersheds. The sorption contributions of HFr fractions are generally higher in sediments than in soil and dust samples. A similar trend was also observed in the distribution of native PAHs between the two fractions (Figure C6). This suggests that relatively more PAHs are concentrated in HFr as well as CMs when they are carried by particles, transported from land surface to the lake, and buried in sediments.

The facts that the majority of the total PAHs are preferentially associated with heavy particles in pavement dust, soils, and sediments, and they tend to concentrate more in heavy particles during transport have potential implications for sediment management.

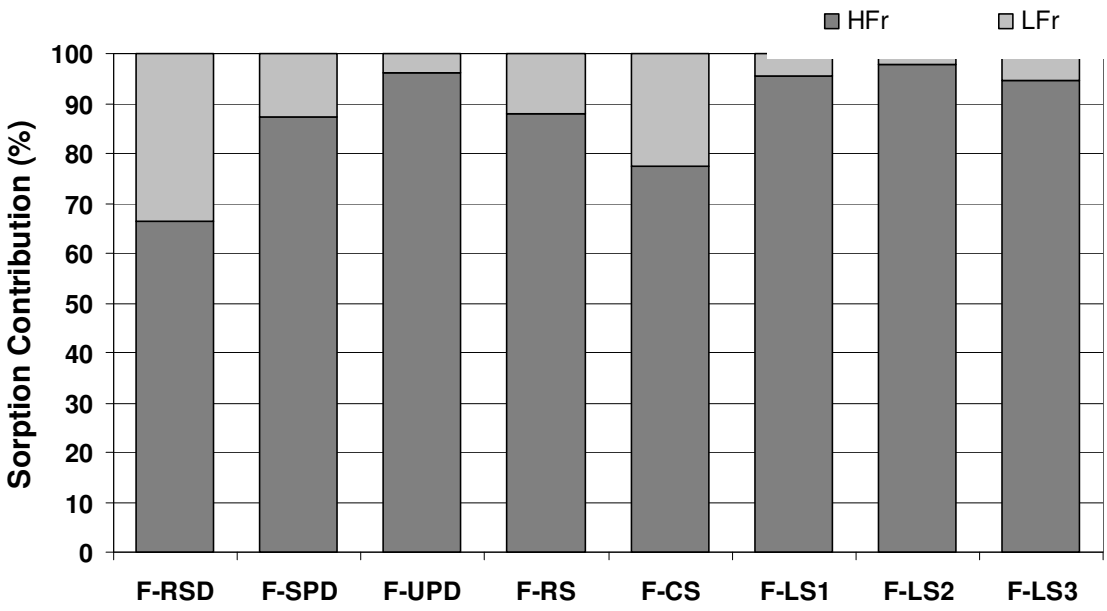

Figure C7. Relative sorption contribution of LFr and HFr fractions of Fosdic Lake watershed samples at an equilibrium concentration of Ce = 10 ug/L.

References

(1) Wilson, J.T., P.C. Van Metre, C.J. Werth, Y. Yang, 2006, Particle-associated contaminants in street dust, parking lot dust, soil, lake- bottom sediment, and suspended and streambed sediment, Lake Como and Fosdic Lake watersheds, Fort Worth, Texas, 2004 U.S. Geological Survey Data Series 211. Denver, CO, U.S. Geological Survey http://pubs.usgs.gov/ds/2006/211/ (accessed May 2009)**,** 24pp.

(2) MacDonald, D.D., C.G. Ingersoll, T.A. Berger, 2000, Development and evaluation of consensus-based sediment quality guidelines for freshwater ecosystems, Archives of Environmental Contamination and Toxicology, 39, 20-31.

(3) Rockne, K.J., L.M. Shor, L.Y. Young, G.L. Taghon, D.S. Kosson, 2002, Distributed sequestration and release of PAHs in weathered sediment: The role of sediment structure and organic carbon properties, Environmental Science & Technology, 36, 2636-2644.